

Scuola Nazionale "Rivelatori ed Elettronica per Fisica delle Alte Energie,
Astrofisica, Applicazioni Spaziali e Fisica Medica"

INFN Laboratori Nazionali di Legnaro
15-19 Aprile 2013

Caratteristiche radiobiologiche dei fasci di ioni e loro impiego in applicazioni adroterapiche

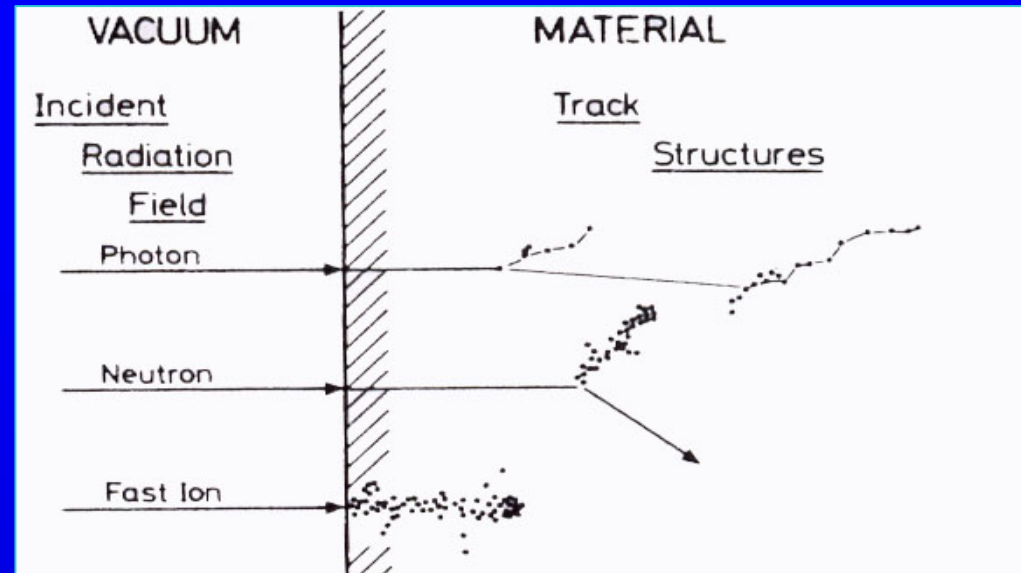
Roberto Cherubini
INFN-Laboratori Nazionali di Legnaro
Legnaro-Padova, Italy

Legnaro, 19 Aprile 2013

Radiation-Matter Interaction

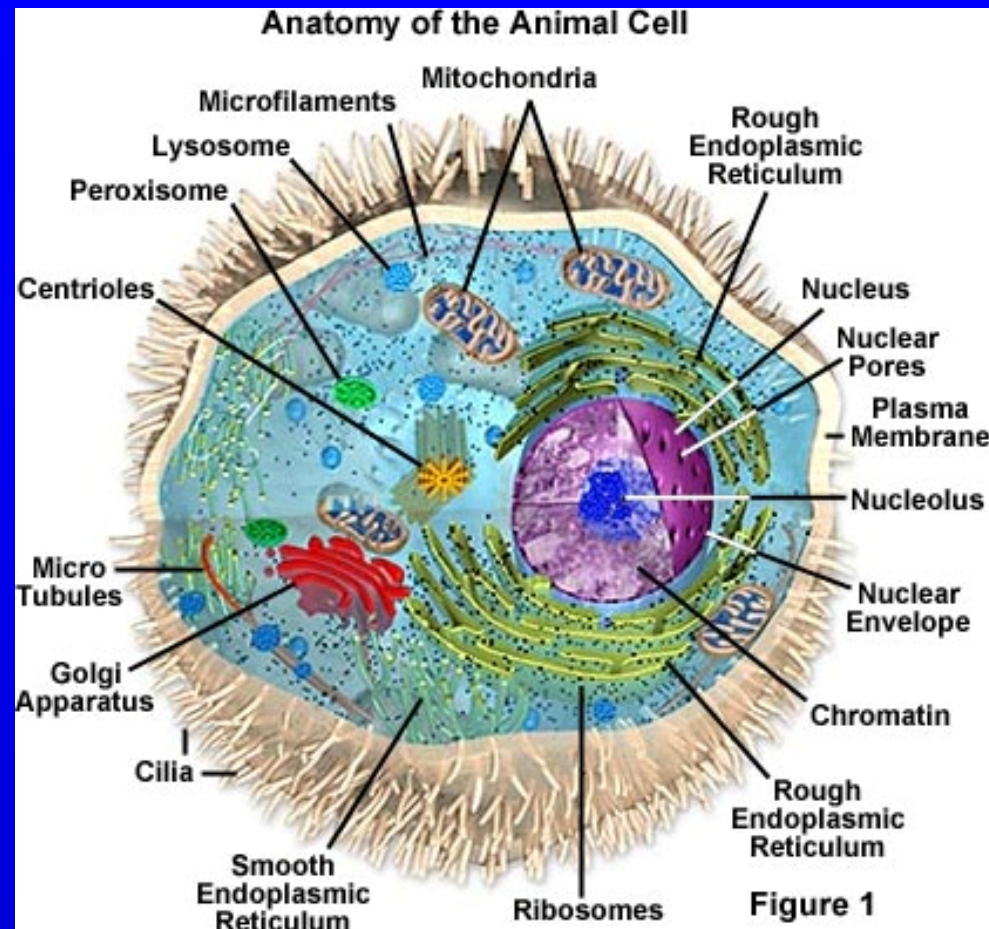
Indirectly Ionizing Radiations

Directly Ionizing Radiations



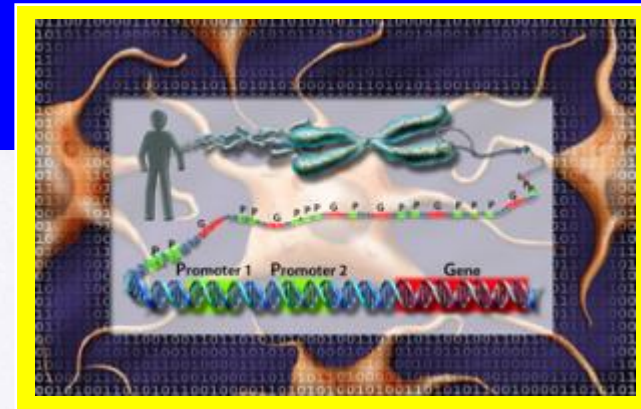
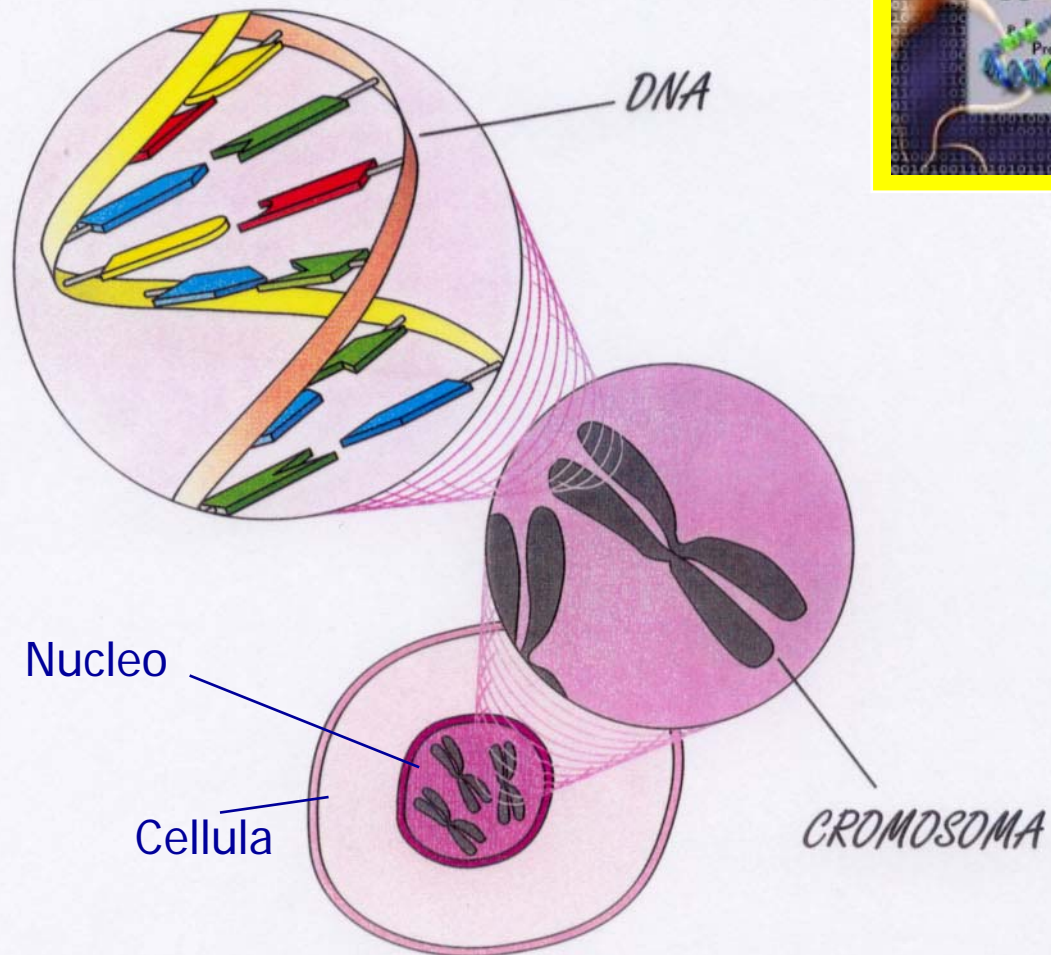
→ but also: Low- and High-LET radiations; or Sparsely and Densely Radiations

...the Target...



Conventionally: the cellular target for radiations is the DNA in the cell nucleus
*...but new/recent evidences at low-dose levels question such an assumption (i.e.:
..non-targeted, non-linear effects..)*

...the Target...



*Nelle cellule in divisione il materiale genico si compatta e divengono visibili i cromosomi.
I cromosomi di una cellula si possono ordinare per numero, dimensioni e forma (cariotipo).*

"Organizzazione" del DNA... I cromosomi

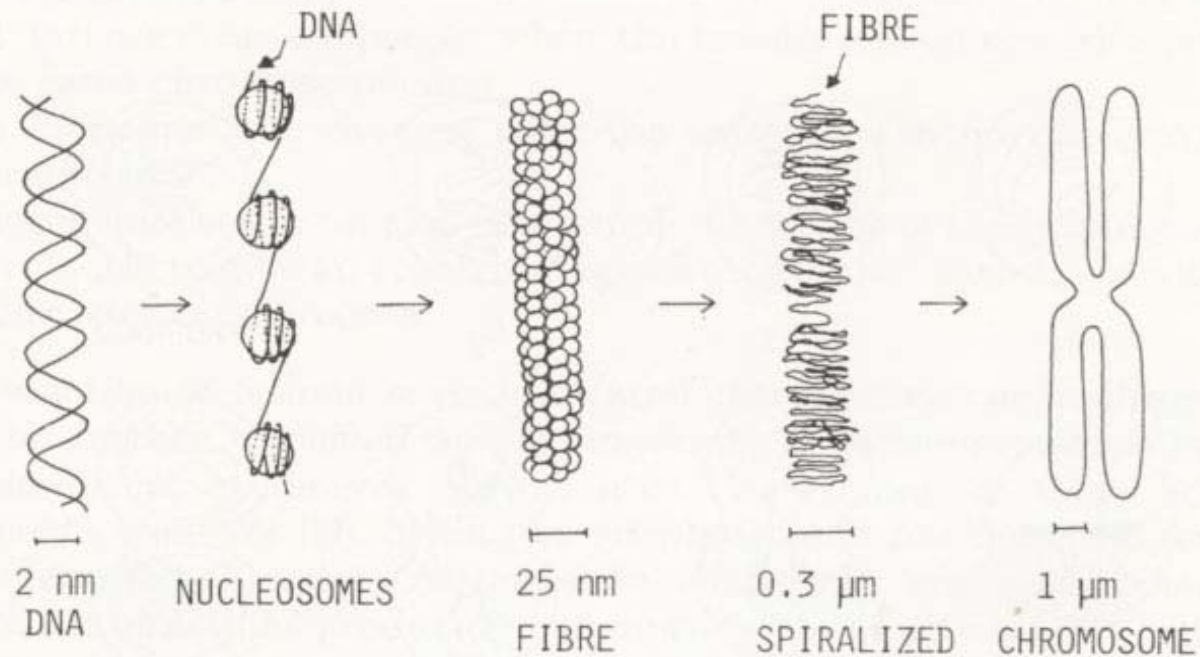


Figure 7.2. Diagram of the molecular organisation of DNA in chromosomes and its association with histone discs (nucleosomes) that form the single fibre running from one end of the chromosome to the other

Source: K. H. Chadwick and L. P. Leenhouts, 1981, *Molecular Theory of Radiation Biology*, Springer-Verlag; courtesy the authors and publisher.

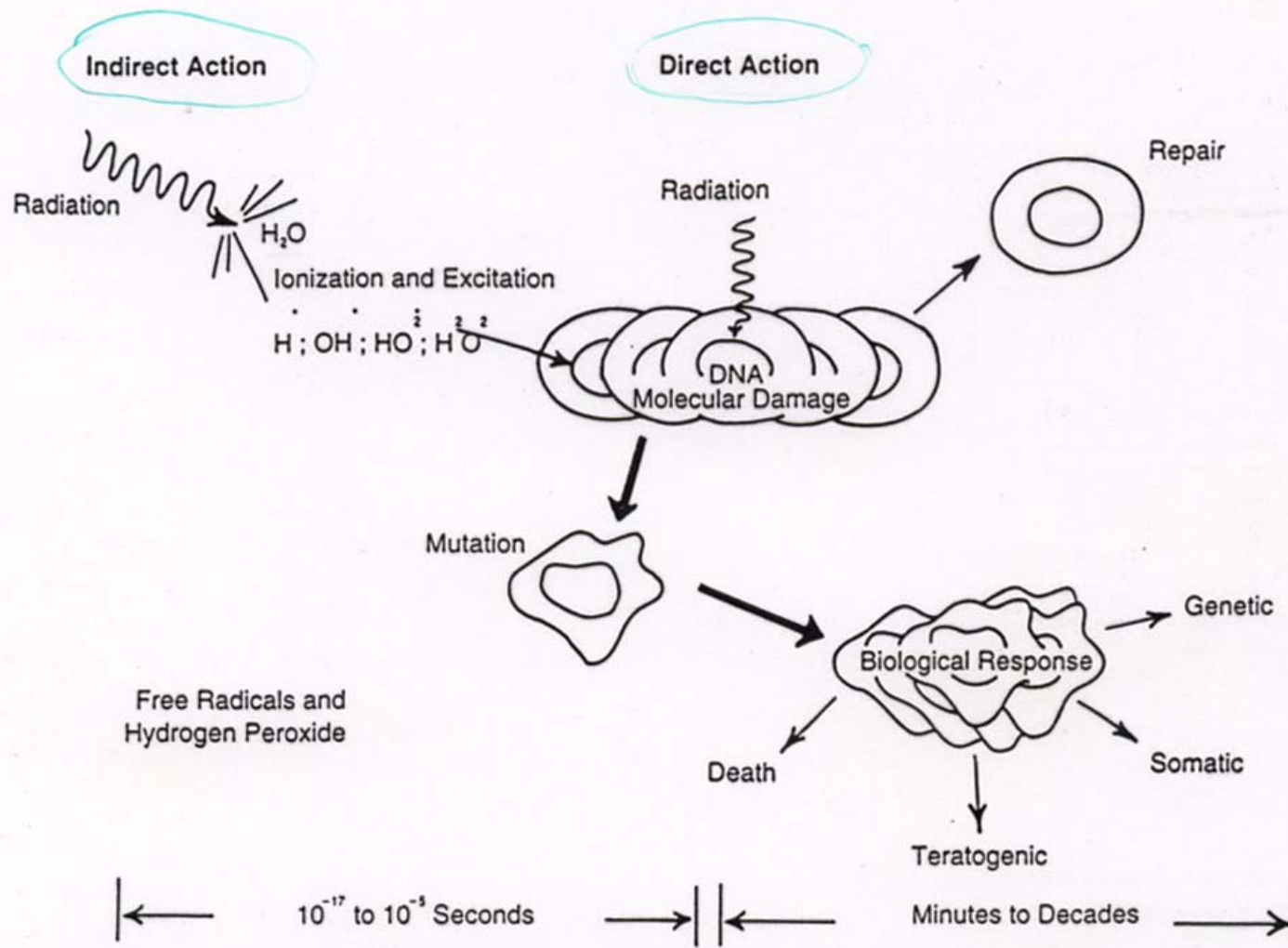


FIGURE 2-24. Direct and indirect action of radiation. [From Bushberg, J.T., Seibert, J.A., Leidholdt Jr, E.M., & Boone, J.M. (1994). *The essential physics of medical imaging*. Baltimore: Williams & Wilkins. Reproduced by permission.]

Table 1.3. Chain of events leading to radiation injury

<i>Event</i>	<i>Timescale</i>
1. <i>Initial interactions</i>	
Indirectly ionizing radiation ^a	10 ⁻²⁴ – 10 ⁻¹⁴ s
Directly ionizing radiation ^b	10 ⁻¹⁶ – 10 ⁻¹⁴ s
2. <i>Physico-chemical stage</i>	
Energy deposition as primary track structure ionizations	10 ⁻¹² – 10 ⁻⁸ s
3. <i>Chemical damage</i>	
Free radicals, excited molecules to thermal equilibrium	10 ⁻⁷ s – hours
4. <i>Biomolecular damage</i>	
Proteins, nucleic acids, etc.	ms – hours
5. <i>Early biological effects</i>	
Cell death, animal death	hours – weeks
6. <i>Late biological effects</i>	
Cancer induction, genetic effects	years – centuries

^a X-rays, γ rays, neutrons

^b Electrons, protons, α particles

....Radiobiological quantities...

Dose (ICRU 51):

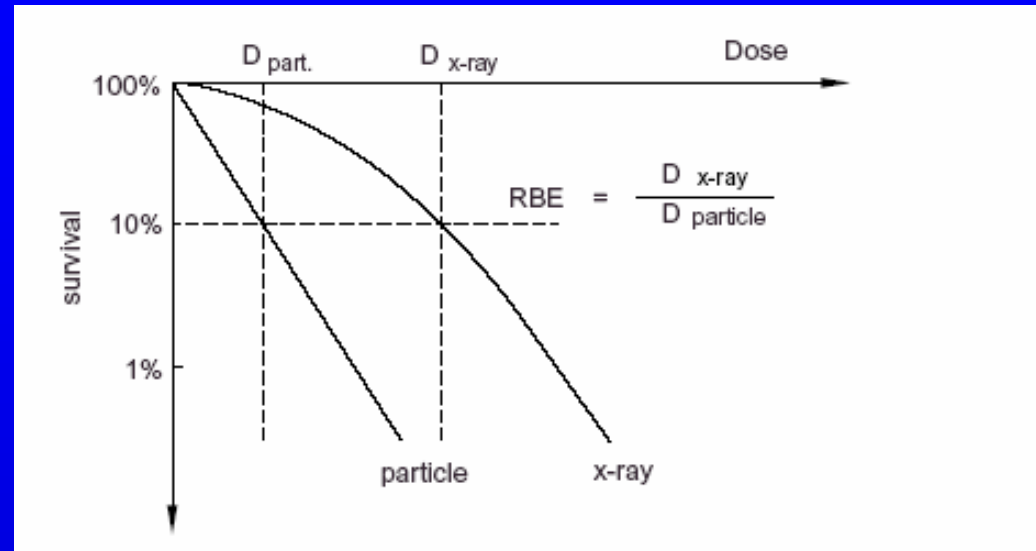
$$D = \frac{d\bar{\varepsilon}}{dm} \quad \text{J/kg, Gy}$$

Dose rate (ICRU 51):

$$\dot{D} = \frac{dD}{dt} \quad \text{Gy/min}$$

Linear Energy Transfer (Zirckle, 1952)

$$LET = \frac{dE}{dx} \quad \text{keV}/\mu\text{m}$$

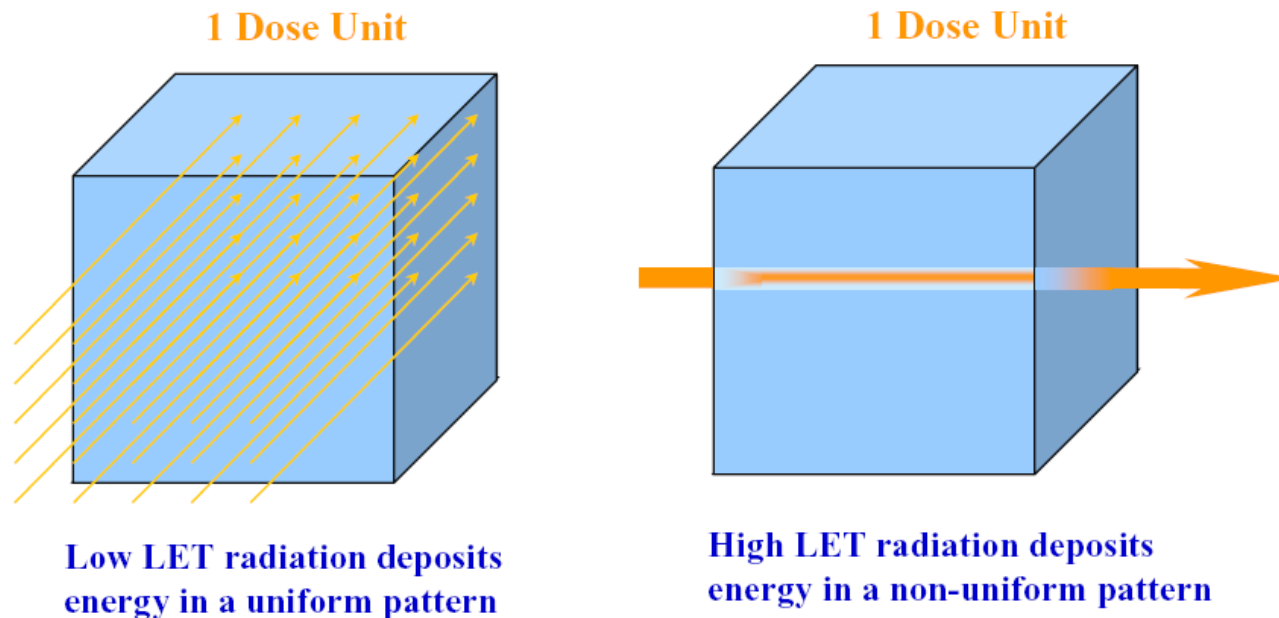


Definition of the relative biological effectiveness, RBE, illustrated for cell survival curves

→ RBE value depends on a variety of factors

The Fundamental Concept of Dose Can Be Fallacious

- ◆ Dose is defined as energy absorbed per unit mass
(irrespective of the spatial distribution of the absorbed energy)



12/6/2000

Neuroscience & Radiobiology Workshop G Nelson

....Energy deposition in matter...

The energy loss as function of particle energy and atomic number is given in the Bethe-Bloch-formula (*Bethe 1930, Bloch 1933*):

$$\frac{dE}{dx} = \frac{4\pi e^4 Z_{eff}^2 N}{m_e v^2} \ln \frac{2m v^2}{I(1-\beta^2)} + \text{relativistic}$$

where:

m_e is the electron mass,

v the projectile velocity,

N the density of the electrons of the target material

e the elementary charge and

β the velocity relative to that of light (v/c)

I the mean ionisation potential.

Z_{eff} the particle effective charge (*empirically approximated by Barkas, 1963*)

$$Z_{eff} = Z \left[1 - \exp \left(- 125 \beta \cdot Z^{-2/3} \right) \right]$$

For high energies, all electrons are stripped off the projectile and the effective charge equals the atomic number.

At lower energies, electrons are collected from the target and the effective charge decreases, yielding zero when the particles stop.

The change of Z_{eff} is the main reason for the sharp decrease of the energy loss at lower/stopping energies

Stopping Power (SP) e Linear Energy Transfer (LET)

- SP: energia totale trasferita dalla particella senza specificare dove sia stata depositata
- LET: energia assorbita **localmente** dal mezzo

Def.: rapporto tra l'energia media dE trasferita localmente dalla radiazione al mezzo, in un tratto dx del suo percorso, e la lunghezza dx del tratto stesso

$LET_{\Delta r}$ = LET ristretto in *range* (Δr : particolare range degli e- emessi)

$LET_{\Delta E}$ = LET ristretto in energia (ΔE : determinato intervallo di energia dello spettro degli e- emessi)

→ $SP \equiv LET_{\infty}$
(senza limitazioni sul *range* e sull'energia degli e- prodotti)

→ *LET usato per definire la qualità di una radiazione per quanto riguarda la descrizione degli effetti radiobiologici indotti da RI*

...RBE dependence on...

Physical factors:

Type of radiation
Energy
Dose-rate
Dose fractionation
:
:
:
Beam production
Beam delivery
... etc...

Biological factors:

Biological end-point
Level of expression
Type of cell, tissue, animal
Repair capability
Cell cycle phase
....

Chemical factors:

Oxygen
Sensitizers
Protectives

...Cell Survival Curves...

Clonogenic assay

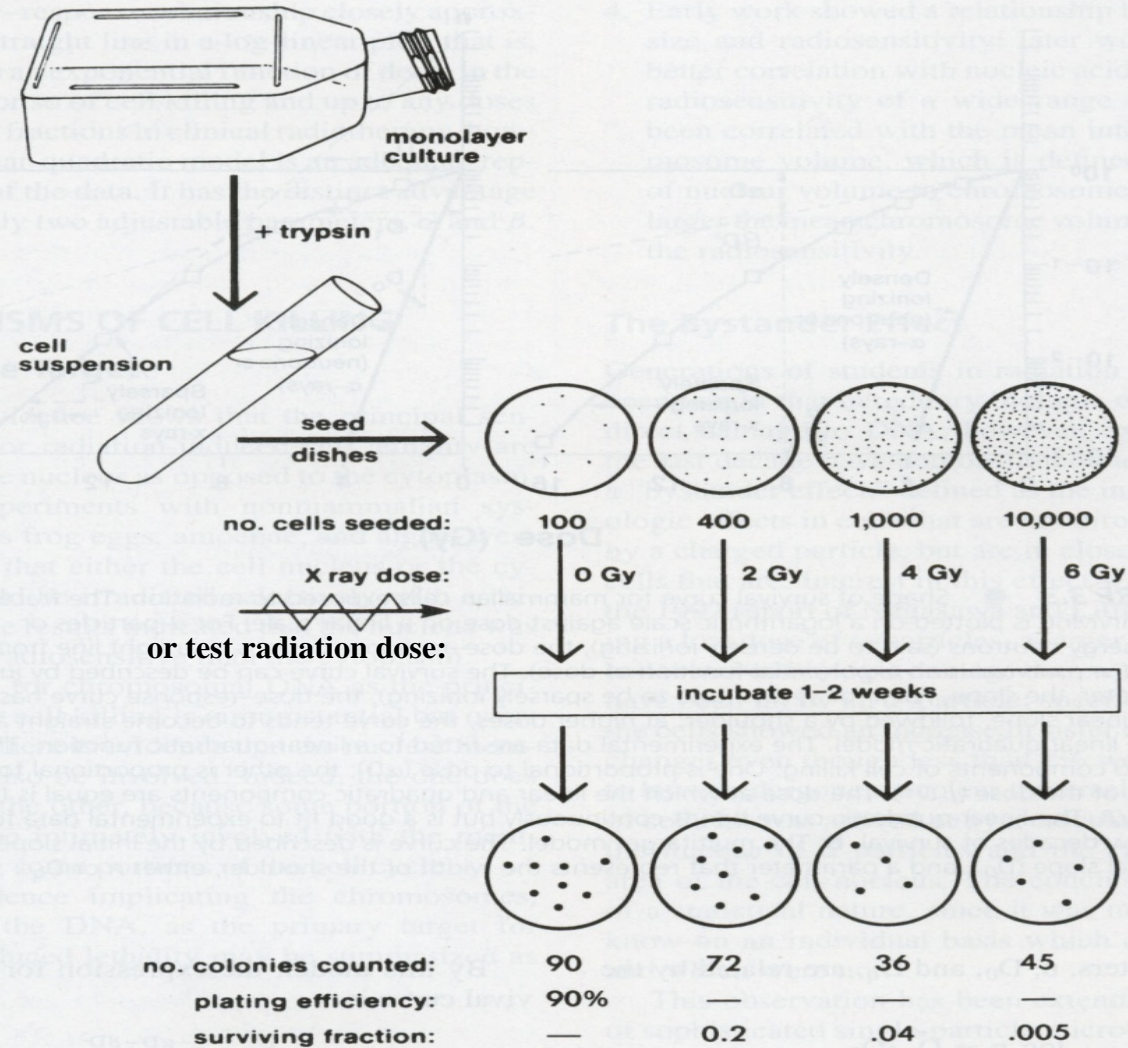
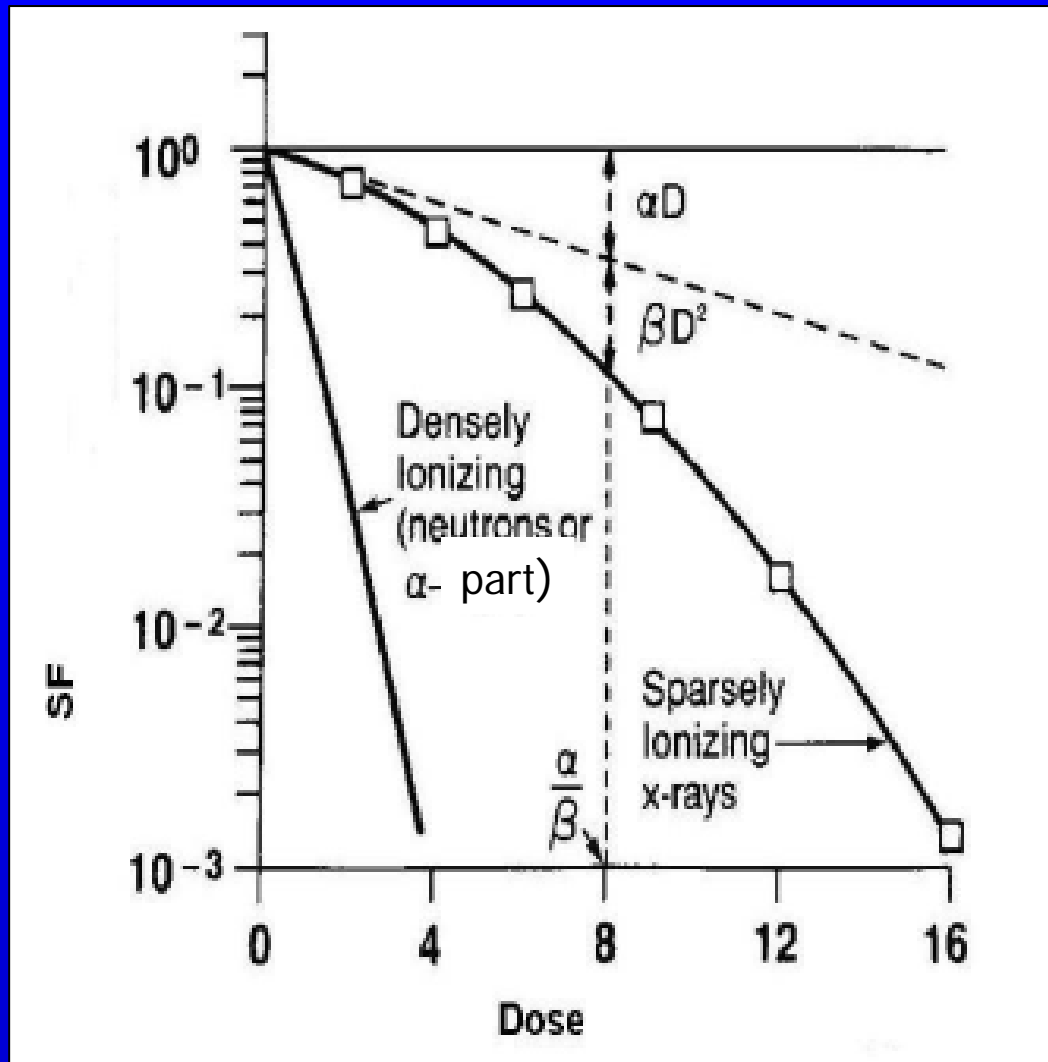


FIGURE 3.2 ● The cell culture technique used to generate a cell survival curve. Cells from a stock culture are prepared into a single-cell suspension by trypsinization, and the cell concentration is counted. Known numbers of cells are inoculated into petri dishes and irradiated. They then are allowed to grow until the surviving cells produce macroscopic colonies that can be counted readily. The number of cells per dish initially inoculated varies with the dose so that the number of colonies surviving is in the range that can be counted conveniently. Surviving fraction is the ratio of colonies produced to cells plated, with a correction necessary for plating efficiency (i.e., for the fact that not all cells plated grow into colonies, even in the absence of radiation).

...Cell Survival Curves...

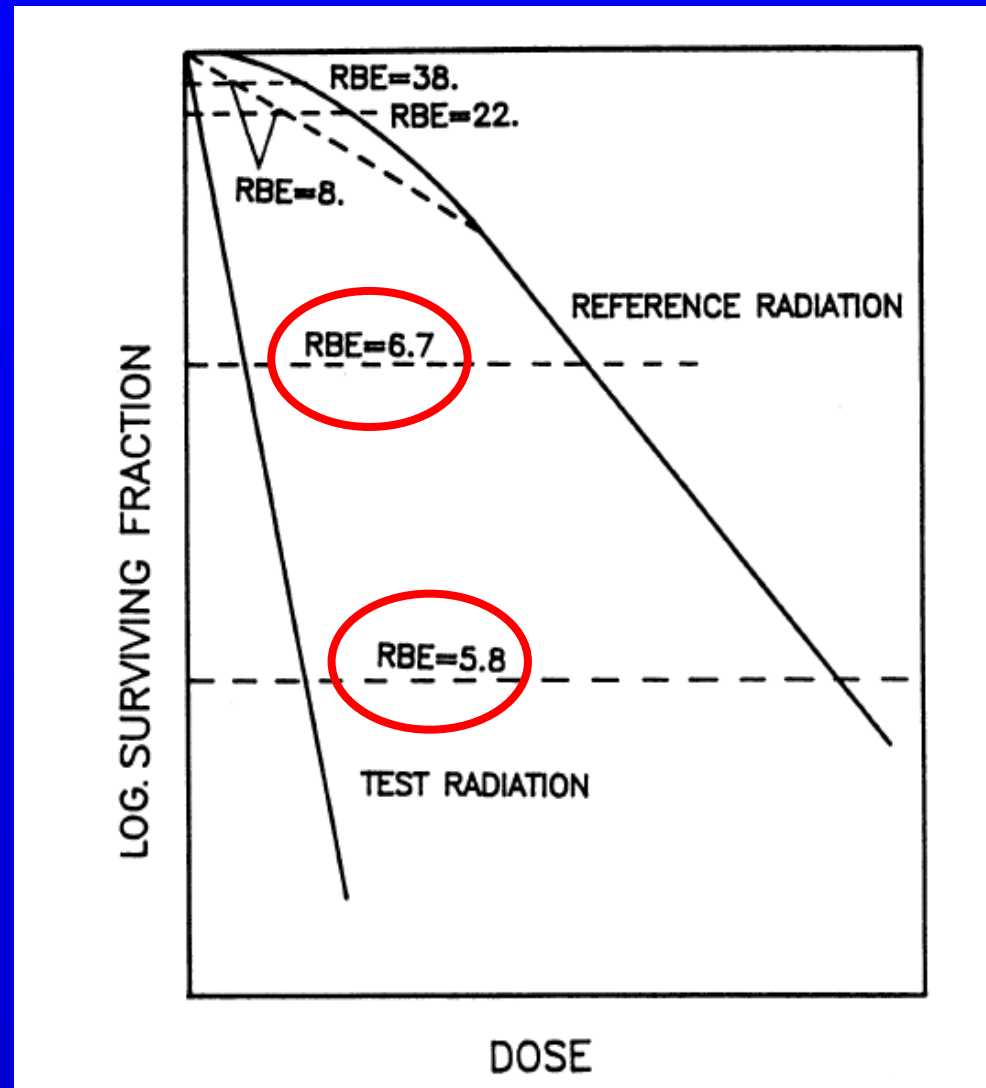


$$SF = \exp(-\alpha D - \beta D^2)$$

$$SF = \exp(-\alpha D)$$

...Cell Survival Curves...

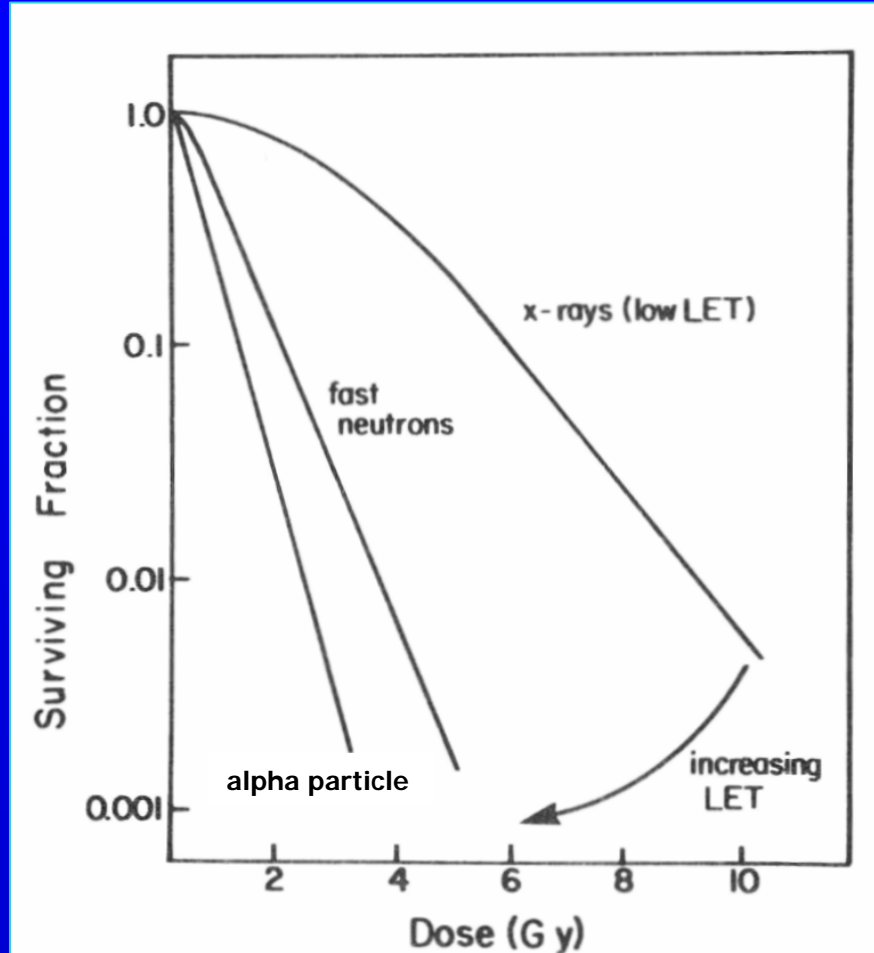
...RBE....



J. Kiefer, 1990

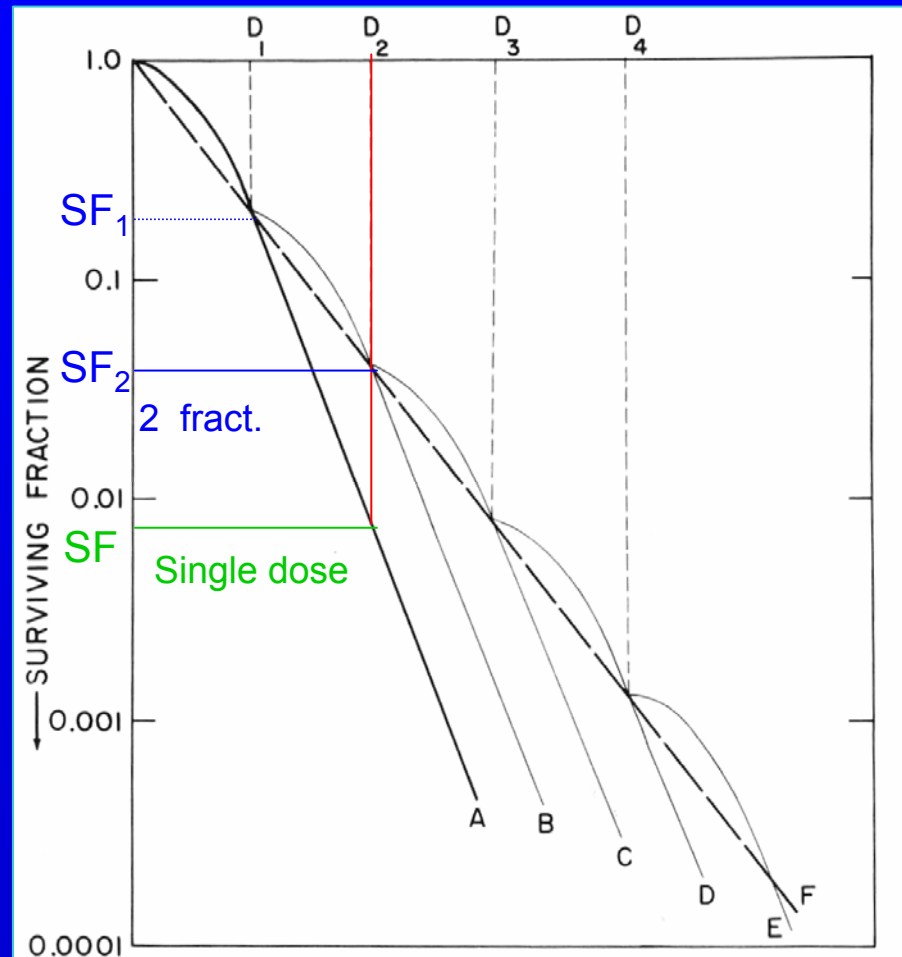
...Cell Survival Curves...

... LET dependence ...



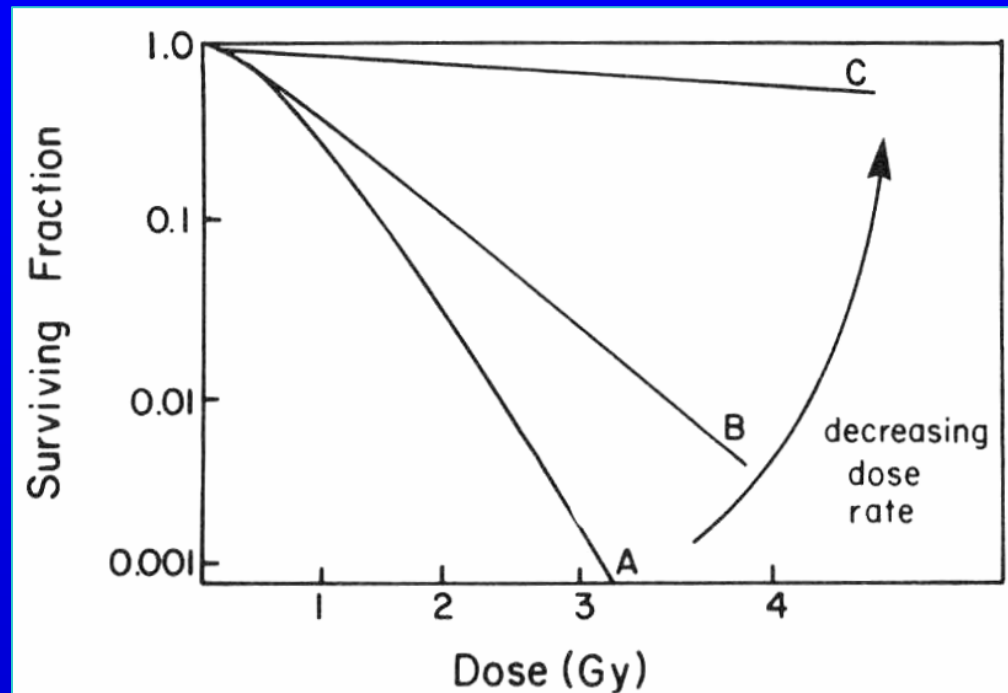
...Cell Survival Curves...

... Dose fractionation ...



...Cell Survival Curves...

...dose-rate effect ...



marked variation for 0.1 Gy/h and 1 Gy/min

...Cell Survival Curves...

... dependence on cell line ...

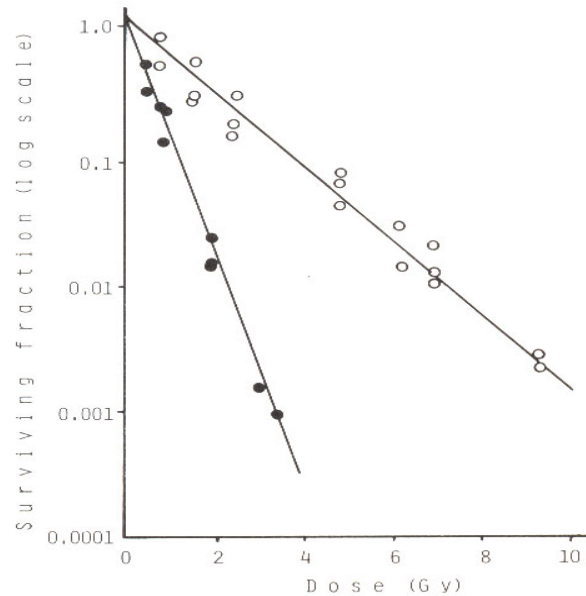
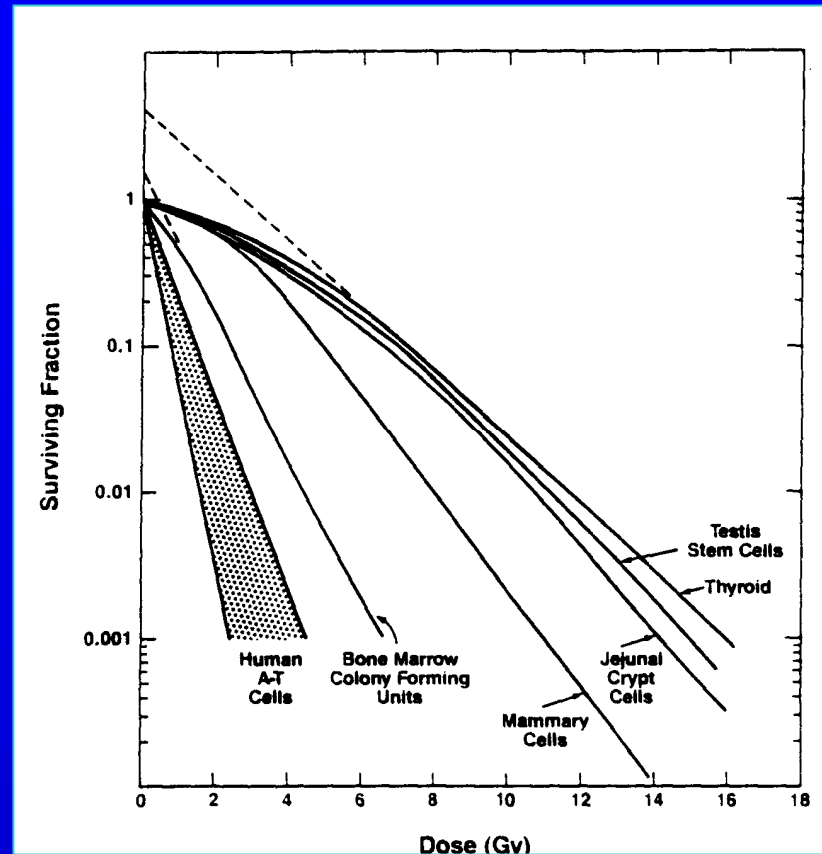
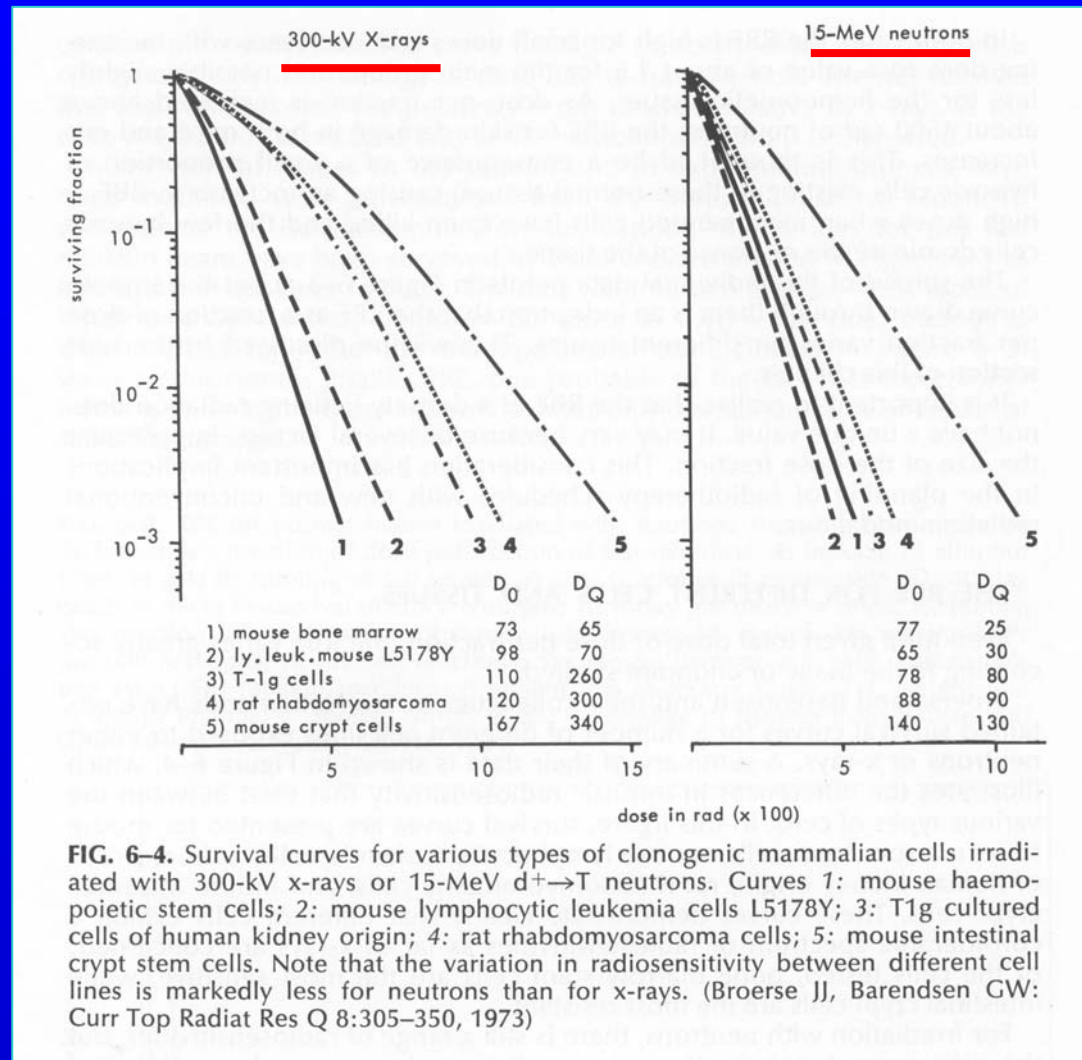


Figure 3.6. X-ray survival curves for human skin fibroblasts from normal patients (○) and from patients with Ataxia telangiectasia (●)
Source: R. R. Weichselbaum, J. Nove and J. B. Little, 1977, *Nature* 266, 726; courtesy the authors and publisher.



...Cell Survival Curves...

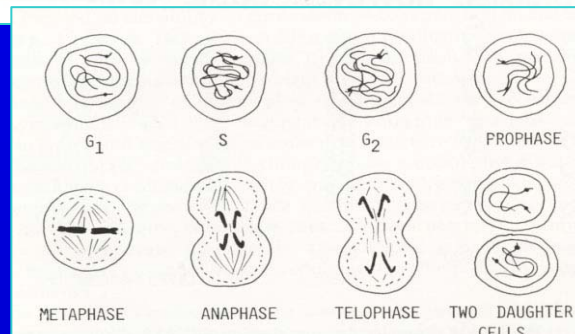
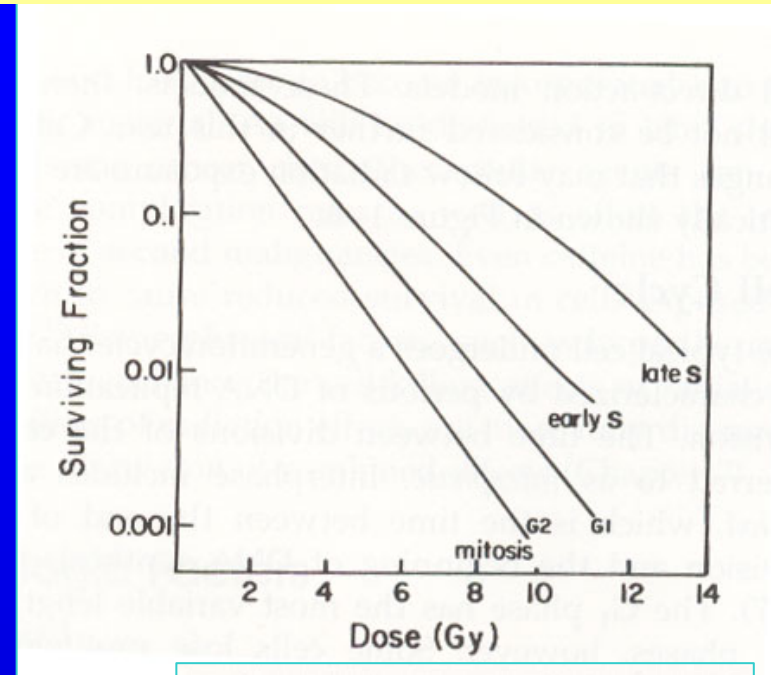
... dependence on cell line ...



...less pronounced for High-LET radiations

...Cell Survival Curves...

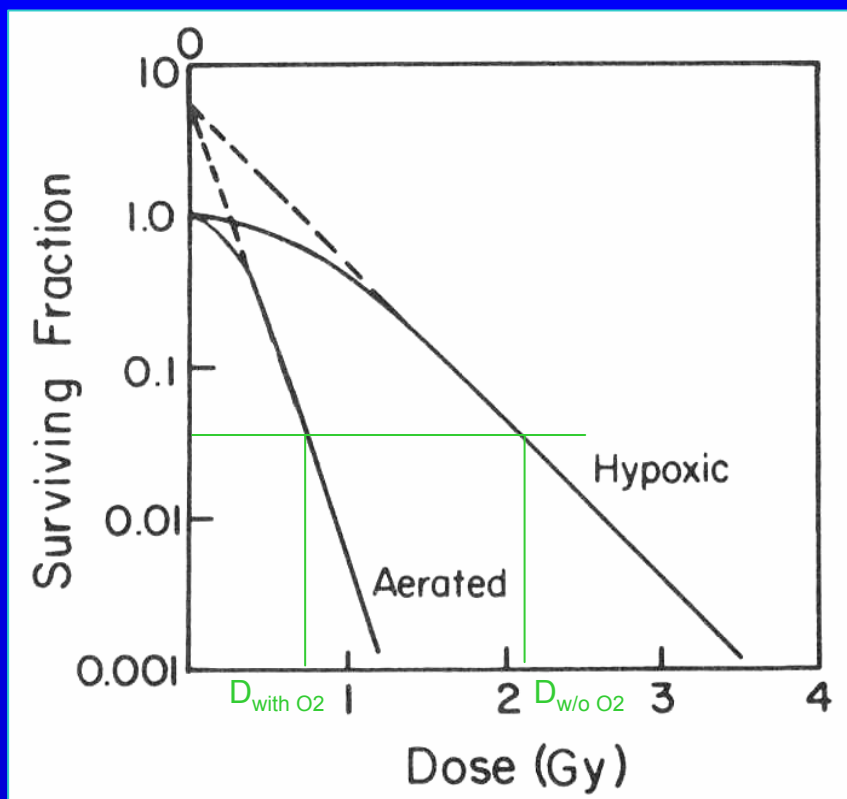
... dependence on cell cycle ...



... less pronounced for High-LET radiations

...Cell Survival Curves...

... Oxygen effect ...



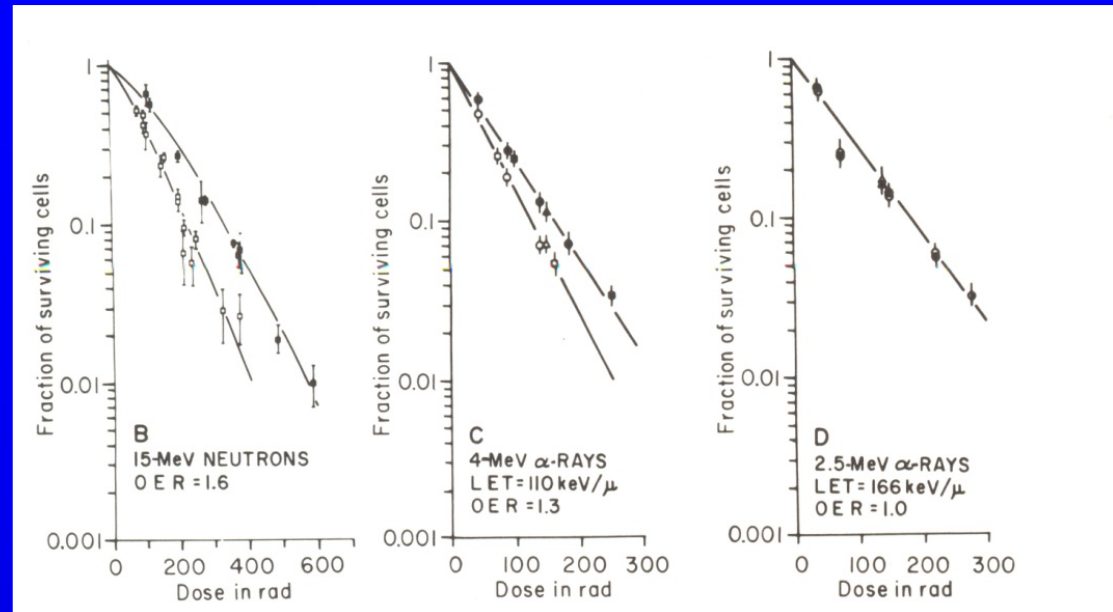
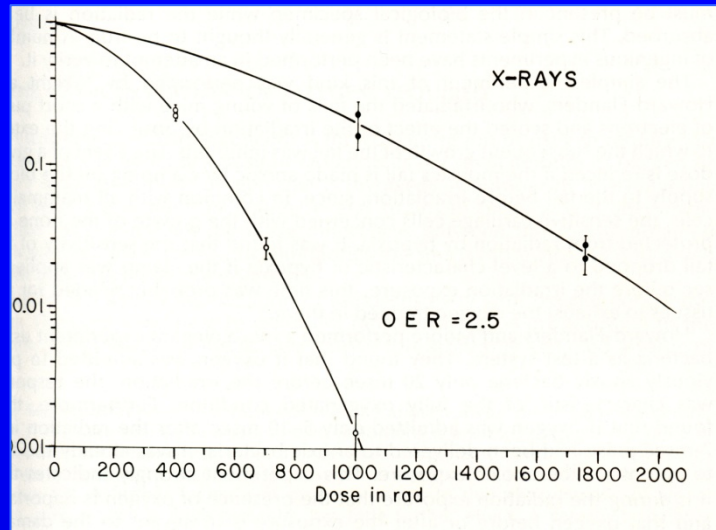
..the oxygen acts as a radiosensitizer.
→ It is a dose-modifying.

It has been introduced the:
“Oxygen enhancement ratio” (OER):

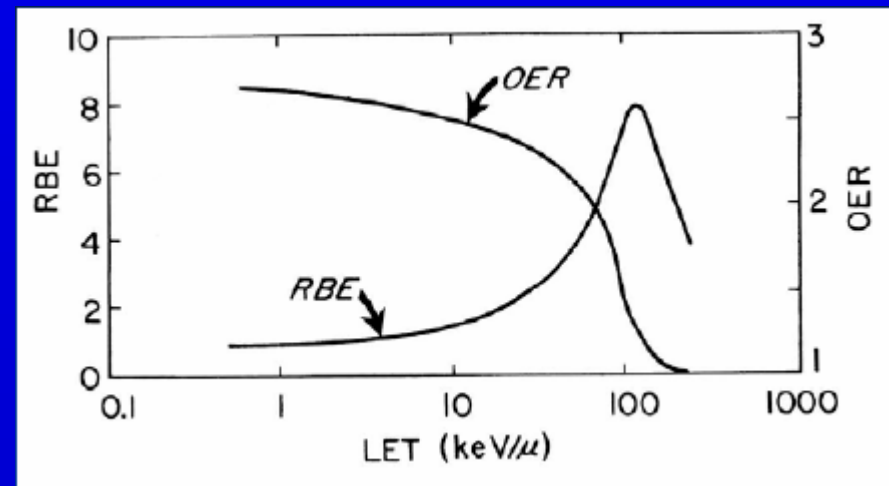
$$\text{OER} = \left[\frac{D_{\text{w/o O}_2}}{D_{\text{with O}_2}} \right]_{\text{iso-effetto}}$$

...less pronounced for High-LET radiations

... Oxygen effect ...



OER~2-3, sparsely ionizing radiations
OER~1, densely ionizing radiations



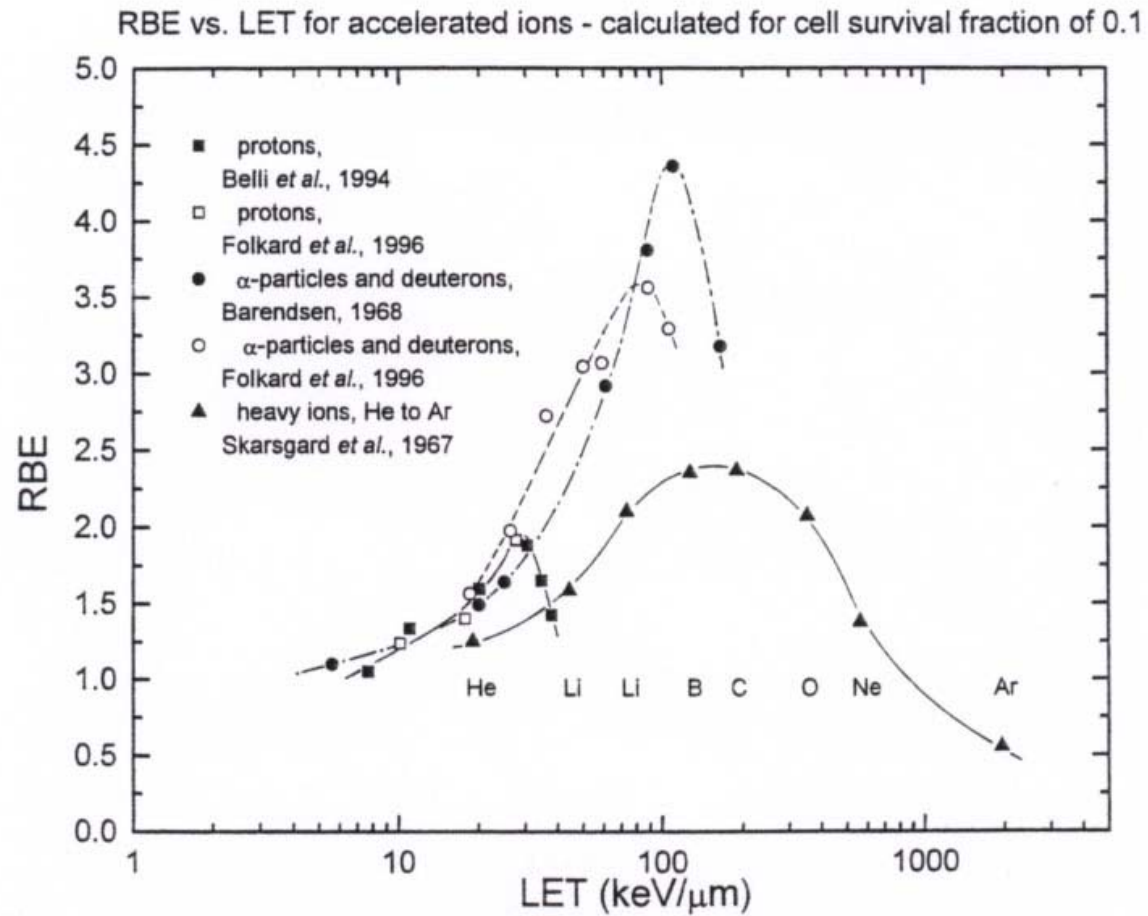
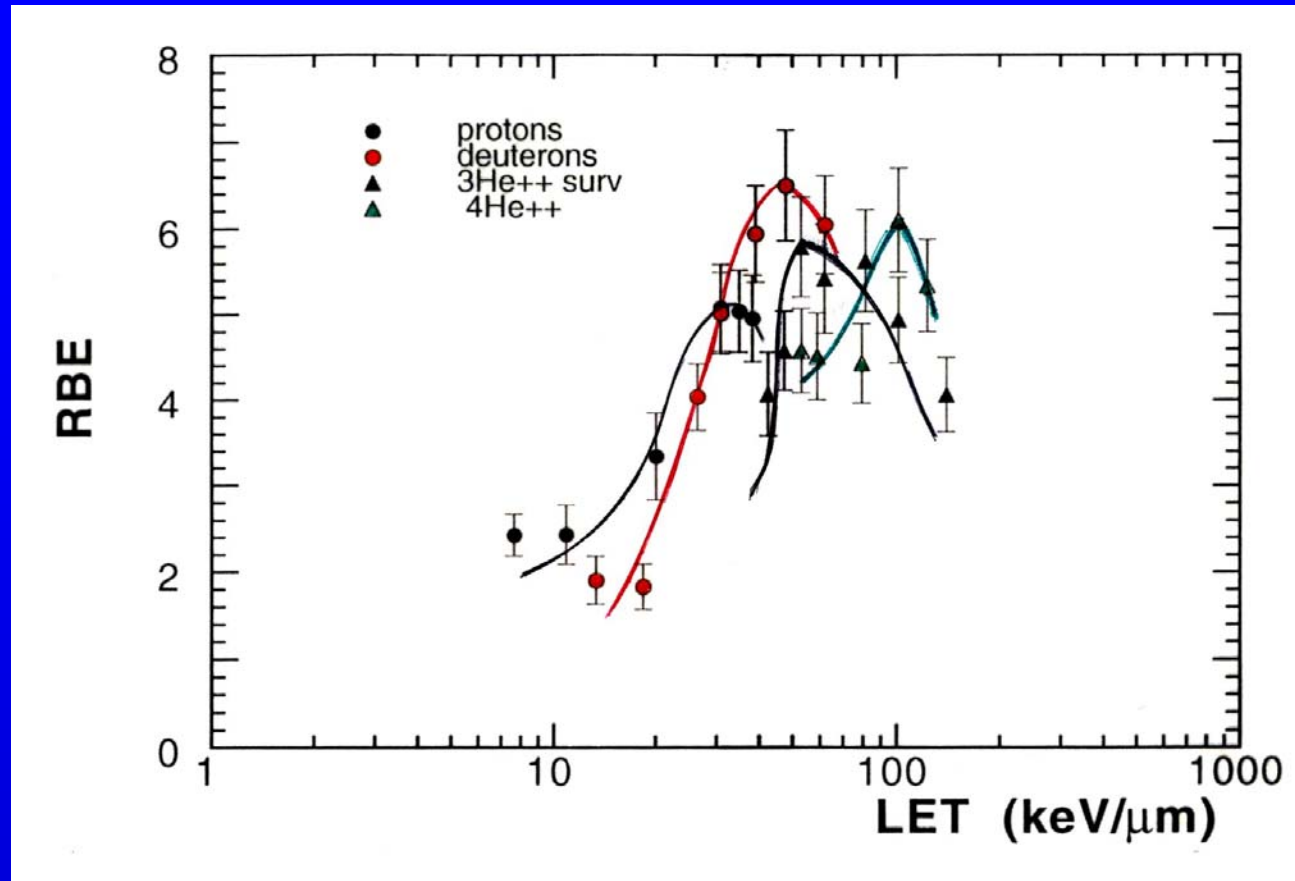


Fig. 10 – Rbe values determined at 10% survival for a variety of accelerated ions of different LET. Cell lines used include V79 (Belli *et al.*, Folkard *et al.*), T-1 (Barendsen) and Ch2B2 (Skarsgard *et al.*).

(Skarsgards, *Physica Medica* 14, Suppl 1,(1998)1-19)

RBE vs LET of Light Charged Particles at LNL-INFN



Relative Biological Effectiveness (RBE) vs Linear Energy Transfer (LET) of light ions for cell inactivation in V79 cells, obtained at the INFN-LNL .

Such results gave the first experimental evidence that low-energy protons are more effective than heavier particles when compared at the same LET values.

(Belli, Cherubini et al, 1989-2000)

RBE, LET e struttura di traccia

- Il parametro LET **non** è indicativo della qualità della radiazione
- Ciò che consente di spiegare la diversa efficacia delle radiazioni è la **struttura di traccia** ...anche se con limiti..

TRACK STRUCTURE THEORY IN RADIOBIOLOGY AND IN RADIATION DETECTION*

ROBERT KATZ

Behlen Laboratory of Physics, University of Nebraska, Lincoln, NE 68588, U.S.A.†

(Received 20 September 1977)

Abstract—The response of biological cells, and many physical radiation and track detectors to ionizing radiations and to energetic heavily ionizing particles, results from the secondary and higher generation electrons ejected from the atoms and molecules of the detector by the incident primary radiation. The theory uses a calculation of the radial distribution of local dose deposited by secondary electrons (delta-rays) from an energetic heavy ion as a transfer function, relating the dose-response relation measured (or postulated) for a particular detector in a uniform radiation field (gamma-rays) to obtain the radial distribution in response about the ion's path, and thus the structure of the track of a particle. Subsequent calculations yield the response of the detector to radiation fields of arbitrary quality. The models which have been used for detector response arise from target theory, and are of the form of statistical models called multi-hit or multi-target detectors, in which it is assumed that there are sensitive elements (emulsion grains, or biological cell nuclei) which may require many hits (emulsion grains) or single hits in different targets (say, cellular chromosomes) in order to produce the observed end-point. Physically, a hit is interpreted as a 'registered event' caused by an electron passing through the sensitive site, with an efficiency which depends on the electron's speed. Some knowledge of size of the sensitive volume and of the sensitive target is required to make the transition from gamma-ray response to heavy ion response. Critical differences in the pattern of response of biological systems and physical detectors to radiations of different quality arise from the number of electrons which must pass through the sensitive volume to produce the recorded end-point. For biological cells this is typically 2 or more. This characteristic multi-hittedness results in survival curves with shoulders, or supralinear dose-response relations for gamma-irradiation, and for an 'RBE' which can exceed 1 at appropriate values of the 'LET'. One-hit detectors cannot mimic the response of biological cells to radiations of different quality. From the beginning it has been clear that SSNTD's (etchable plastics) are not 1-hit detectors. But even now, we do not know their characteristic response to gamma-rays. We are not able to produce a satisfactory theory of track structure in these detectors. There is only a hint, that etching rate is nominally proportional to the quantity z^4/β^4 of the incident ion, suggesting the possibility of a '2-or-more' hit detector.

Recent work has demonstrated that many-hit physical detectors do exist. From both emulsion sensitometry and from the structure of tracks of heavy ions, we are able to show that emulsion-developer combinations exist which yield many-hit response. There is also some evidence that the supralinearity in thermoluminescent dosimeters arises from a mixture of 1-hit and 2-hit response, perhaps of different trap structures within the same TLD crystal. These detectors can be expected to mimic the response of biological cells to radiations of different quality. Their patterns of response may help us to understand better the structure of particle tracks in SSNTD's.

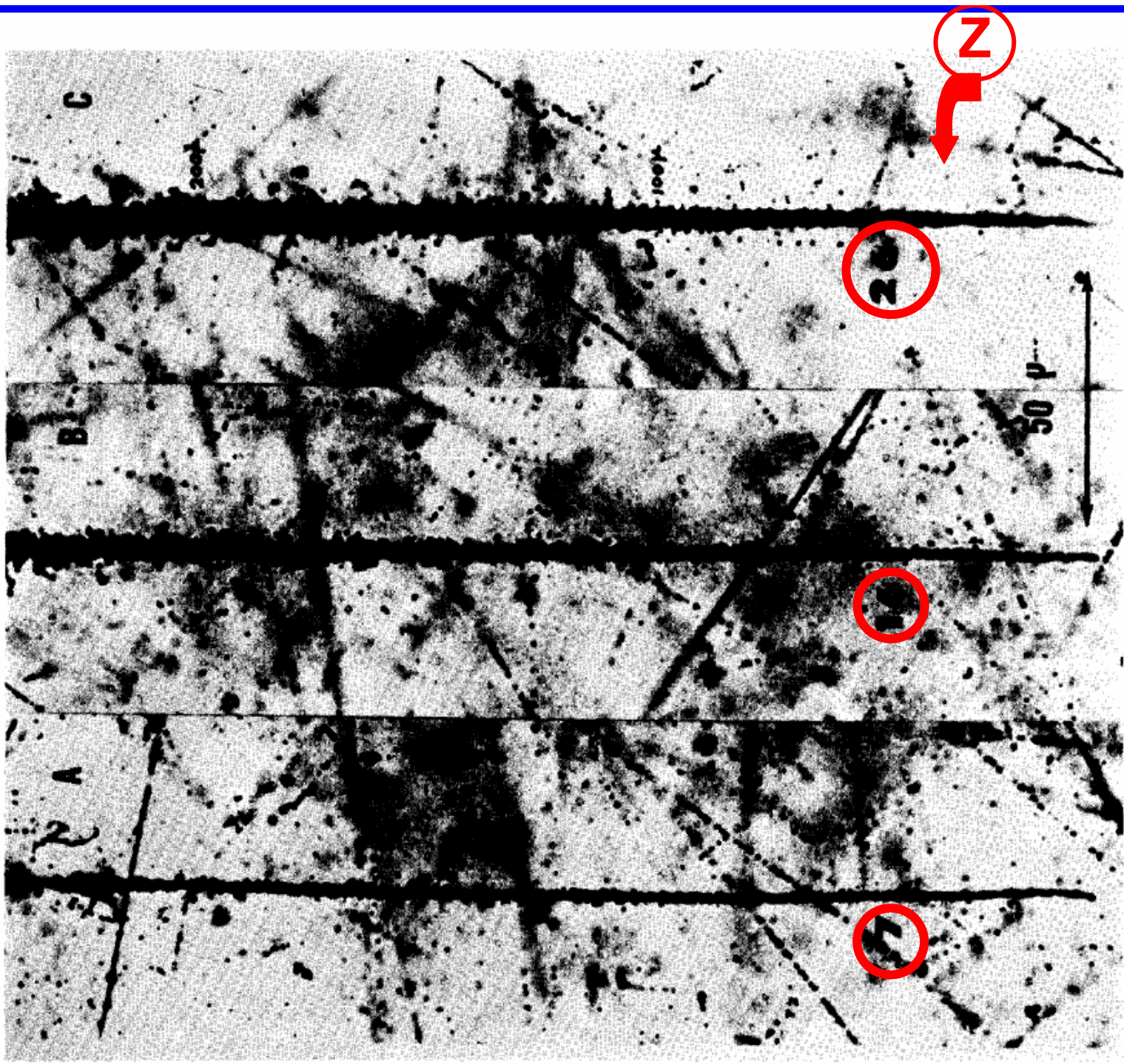
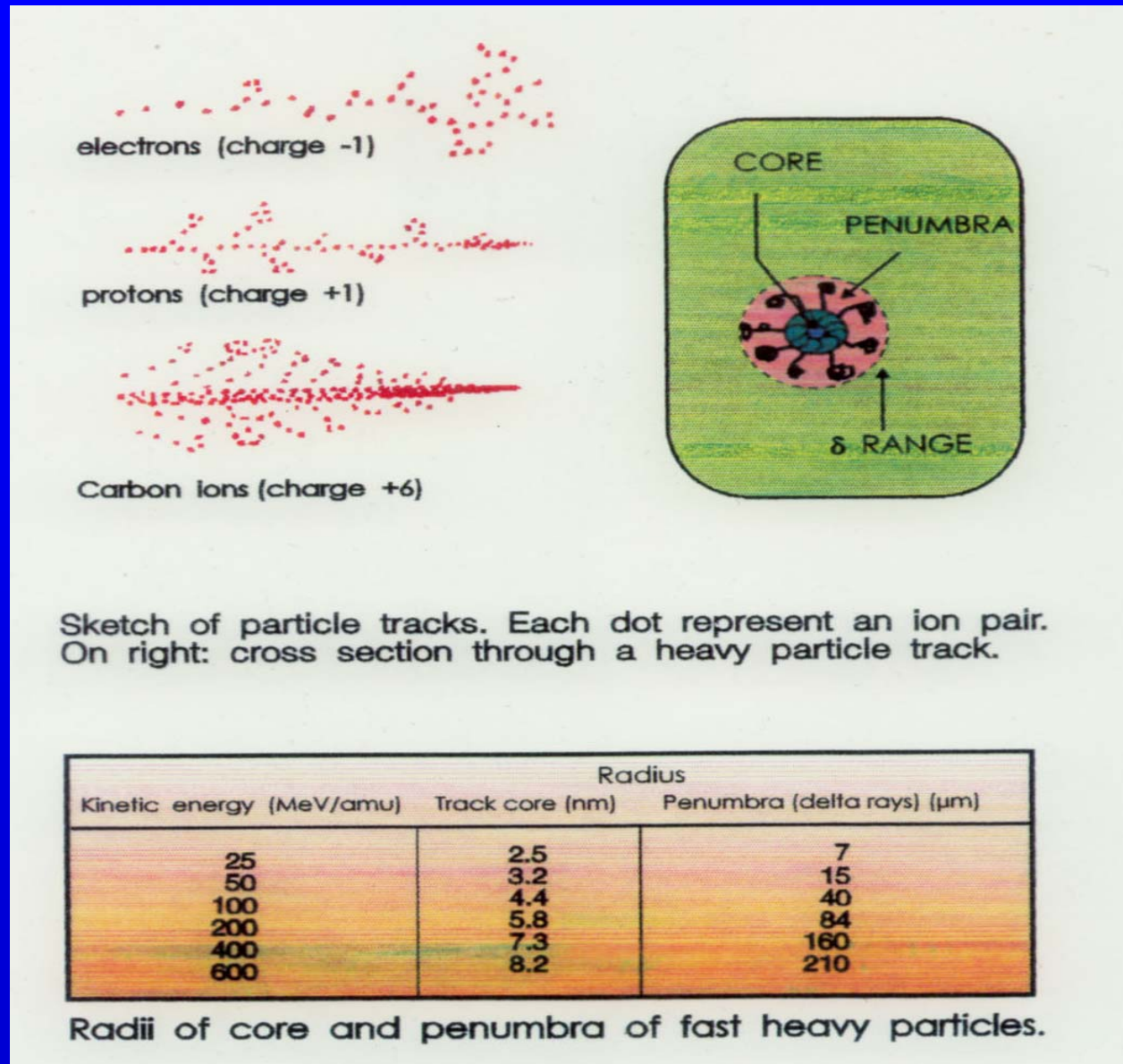


FIG. 15. Stopping tracks of heavy ions in Ilford G.5 emulsion. Courtesy H. Yagoda. The maximum value of the ionization occurs at a residual range from 4 (for $Z = 7$) to 20 (for $Z = 26$) microns.

Microscopically... Particle Track Structure in the matter



Tracks in chromatin fibre

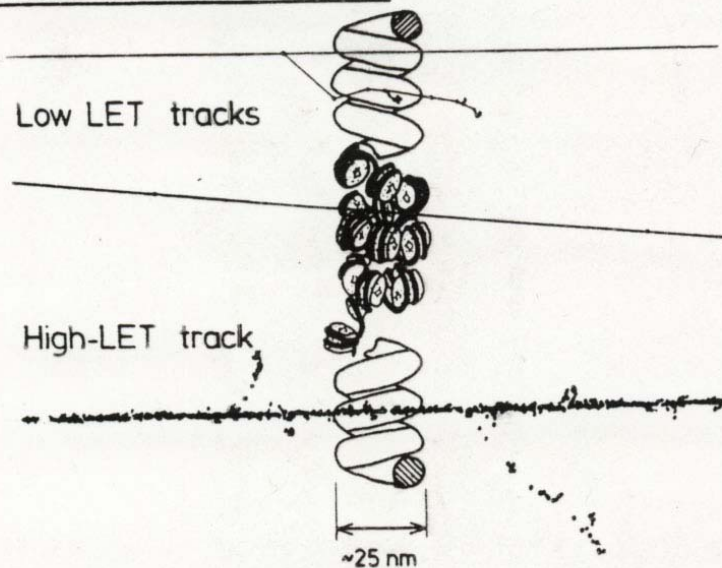
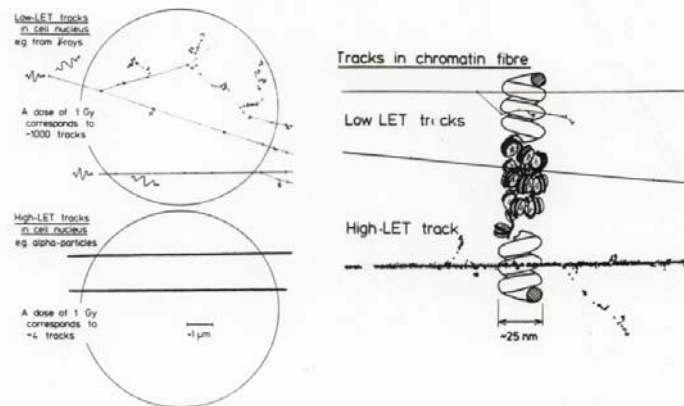
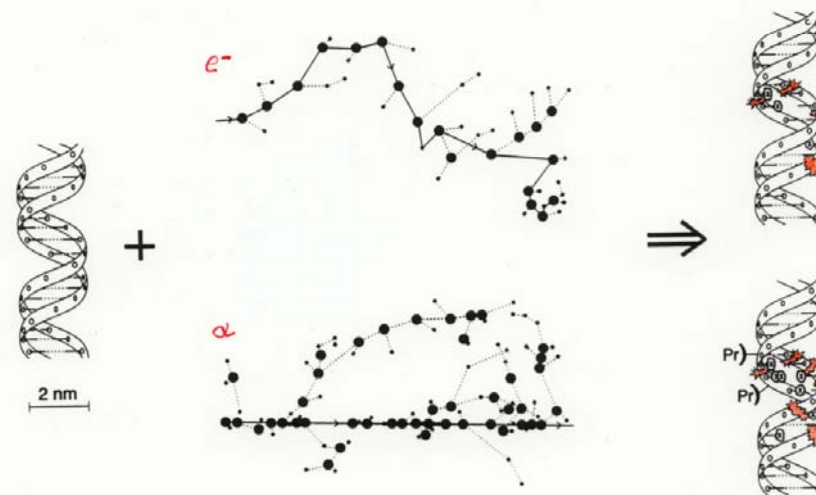


Figure 1-2. Diagram of high- and low-LET tracks passing through a section of chromatin (a mixture of DNA and protein): Low-LET radiation causes relatively sparse ionization along the track of the radiation, whereas high-LET radiation causes very dense ionization along the radiation path with a cluster of radiation at the end of the path (the Bragg peak). Adapted from ICRP: *The 1990 Recommendations of the International Commission on Radiological Protection*. ICRP Pub. No. 60, *Annals of the ICRP*, Oxford, Pergamon Press, 1991.



Schematic representation of (left) a cell nucleus irradiated with two electron tracks from γ -rays (low LET) or two α -particle tracks (high LET). A true scale diagram would require that the clusters of ionizations near the track ends of the low-energy secondary electrons be very much more compact, illustrated (right) on the scale of DNA and chromatin fibre (reproduced from Goodhead 1988).



A segment of DNA drawn on the same scale as two-dimensional projections of an actual simulated low-energy electron track (upper: initial energy 500 eV and coming to rest) and an actual simulated short portion of an α -particle track (lower: energy 4 MeV). Superimposing these tracks randomly onto the DNA suggests that a variety of clustered damages can result: two notional possibilities are illustrated on the right. Broken ribbons indicate DNA strand breaks, X indicates base damage and Pr indicates a DNA-protein cross link. In these track diagrams large circles are ionizations and small circles are excitations.

MICROSCOPIC CONSEQUENCES OF 1 cGy ABSORBED DOSE




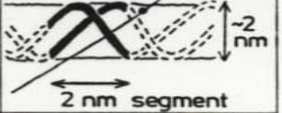

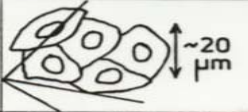
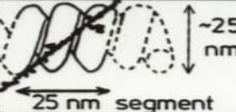


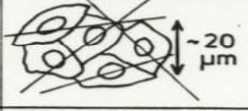


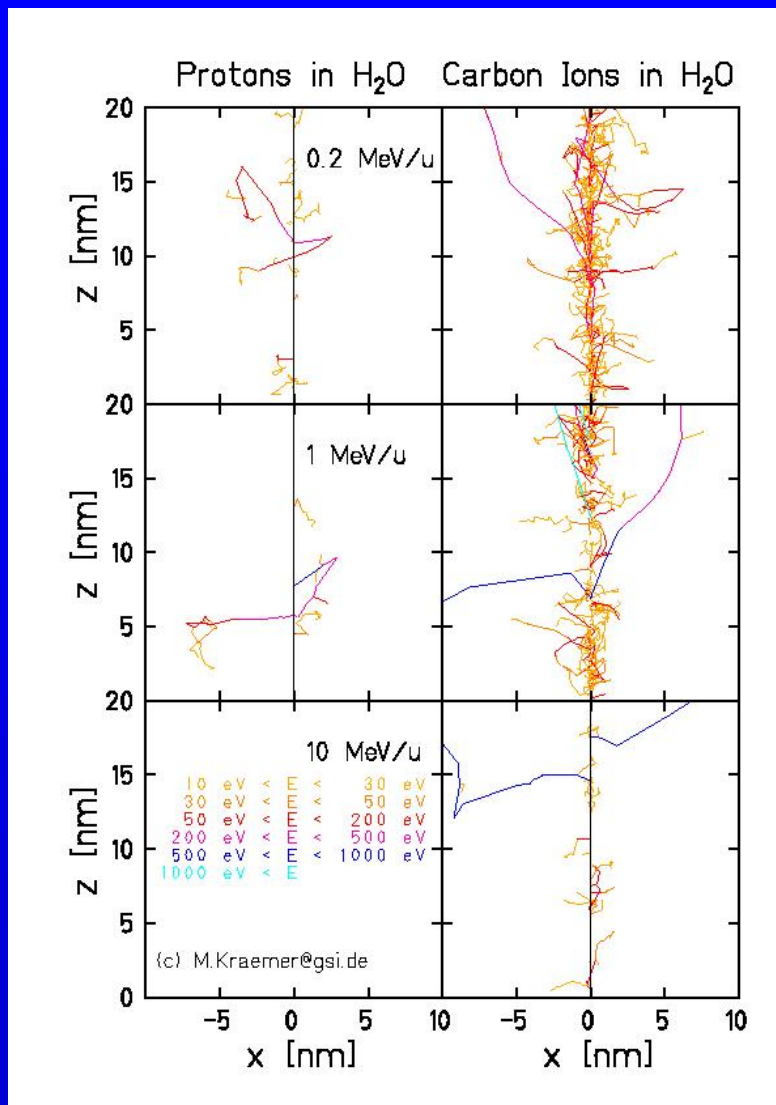
	Whole tissue	Individual cells	Chromatin fibre (total ~5 cm per cell)	DNA (total ~2 m per cell)	Mean number lethal lesions per cell
External γ-rays		 ~20 μm	 ~25 nm 25 nm segment	 ~2 nm 2 nm segment	~0.001
Dose uniformity	Uniform Dose = 1 cGy	~ Uniform Dose = 1 cGy	Very large fluctuations Doses = 0 to $\sim 10^3$ Gy	Very large fluctuations Doses = 0 to $\sim 10^6$ Gy	
Mean number of tracks	10^9 gram $^{-1}$	~ 50 cell $^{-1}$ No cells unirradiated	$\sim 10^{-6}$ segment $^{-1}$ ~20 segments hit cell $^{-1}$	$\sim 10^{-8}$ segment $^{-1}$ ~10 segments hit cell $^{-1}$	
Internal ^{220}Rn (3 α's)		 ~20 μm	 ~25 nm 25 nm segment	 ~2 nm 2 nm segment	~0.01
Dose uniformity	Variable Doses = 0 to ~2 cGy	Large fluctuations Doses = 0 to ~30 cGy	Very large fluctuations Doses = 0 to $\sim 10^4$ Gy	Very large fluctuations Doses = 0 to $\sim 2 \times 10^6$ Gy	
Mean number of tracks	$\sim 10^7$ gram $^{-1}$	~ 0.1 cell $^{-1}$ ~90% of cells unirrad.	$\sim 6 \times 10^{-7}$ segment $^{-1}$ ~1 segment hit cell $^{-1}$	$\sim 10^{-8}$ segment $^{-1}$ ~10 segments hit cell $^{-1}$	
External 10 MeV neutrons		 ~20 μm	 ~25 nm 25 nm segment	 ~2 nm 2 nm segment	~0.005
Dose uniformity	Uniform Dose = 1 cGy	Large fluctuations Doses = 0 to ~5 cGy	Very large fluctuations Doses = 0 to $\sim 5 \times 10^3$ Gy	Very large fluctuations Doses = 0 to $\sim 10^6$ Gy	
Mean number of tracks	$\sim 10^7$ gram $^{-1}$	~ 1 cell $^{-1}$ ~37% of cells unirrad.	$\sim 4 \times 10^{-6}$ segment $^{-1}$ ~8 segments hit cell $^{-1}$	$\sim 10^{-8}$ segment $^{-1}$ ~10 segments hit cell $^{-1}$	

FIG. 1. Diagrammatic representation of microscopic patterns of tracks in tissue irradiated with 10 mGy of dose for three different radiations (low-LET γ rays, high-LET α particles, and mixed-LET fast neutrons). For each radiation the mean numbers of tracks are given for large volumes, corresponding to whole tissues, then for cells, chromatin, and down to the very small volumes of segments of DNA. Also given are the dose uniformity at these four levels of resolution; these are expressed as the range of doses received by individual target volumes. For example, for the 2-nm long segments of DNA only 1 such target volume in 10^8 receives any energy deposition at all; when this does occur the microscopic dose to that segment can have any value up to about 10^6 Gy, depending on the chance interactions of the radiation track as it passes through. The last column illustrates how these different patterns of local energy deposition (in all cases for the same macroscopic average energy deposition or dose, 10 mGy) affect the probability of permanent biological damage to the cell. The quoted values are typical for cell inactivation; much lower probabilities are found for cell transformation, or mutation at a single locus, but the sequence of relative effectiveness of the radiations persists. (From Goodhead, 1987b).

...Energy deposition... and Particle Track Structure in matter...
 ..essential element for the use of heavy particles in tumor therapy...



...**No** difference whether an electron is created by the impact of photon or of a heavy charged particle \Rightarrow ...**No** difference in the biological action of each individual electron either.

.....But:

- Difference in the *spatial distribution* between electrons created *along a track* of a heavy charged particle and the *random distribution* of electrons created by photons
- Difference in ionisation density between particles of different energies and atomic numbers like protons, alphas, carbon ions...

...track structure model...

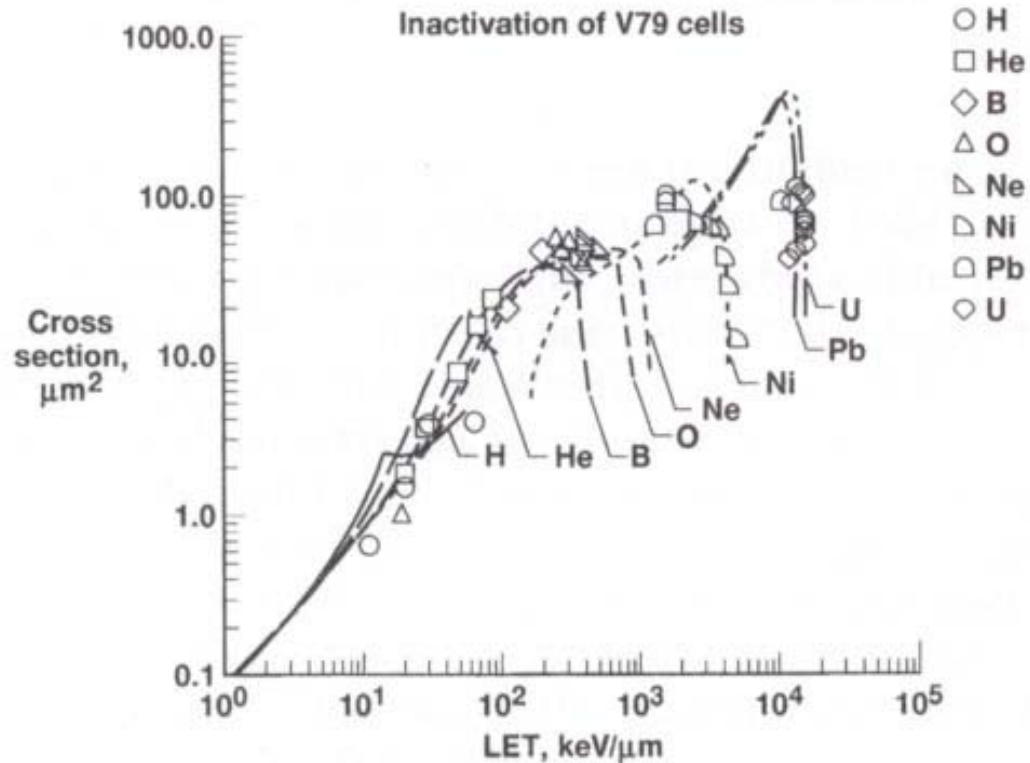
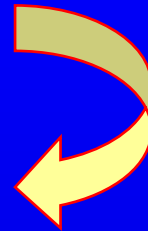


Figure 3. Calculations and experimental values of inactivation cross sections (final slope) for V79 cells plotted versus LET. Data are from Thacker *et al.* (1979), Kranert, *et al.* (1990), Belli *et al.* (1993), and Kiefer *et al.* (1994).

Cucinotta *et, IJRB 69(1996)593*

..but..

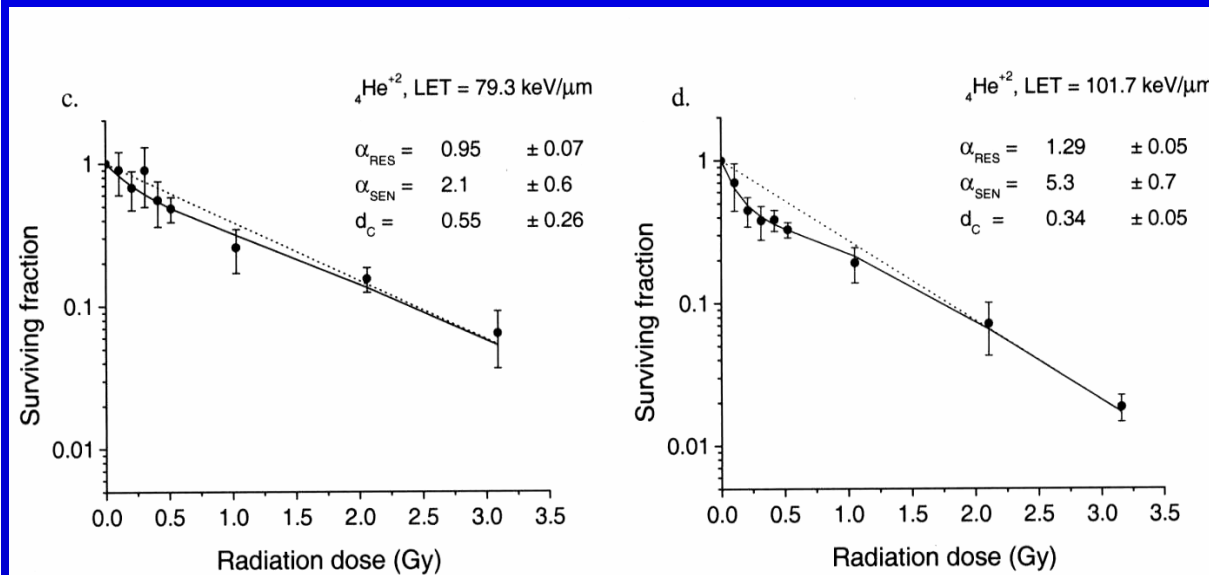
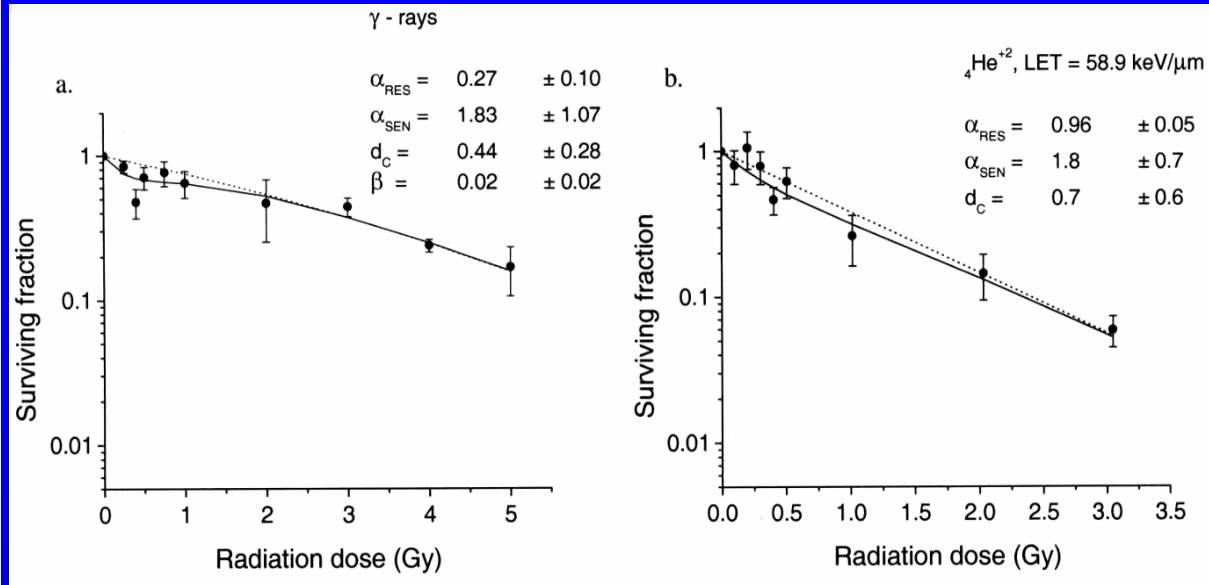
...Low-dose Ionizing Radiation regime...



..evidences for Non-targeted Effects..

Hyper-radiosensitivity and Induced radioresistance

(E. Tsoulou et al., *Int. J. Rad. Biol.* (2001), vol. 77, 1133-1139)

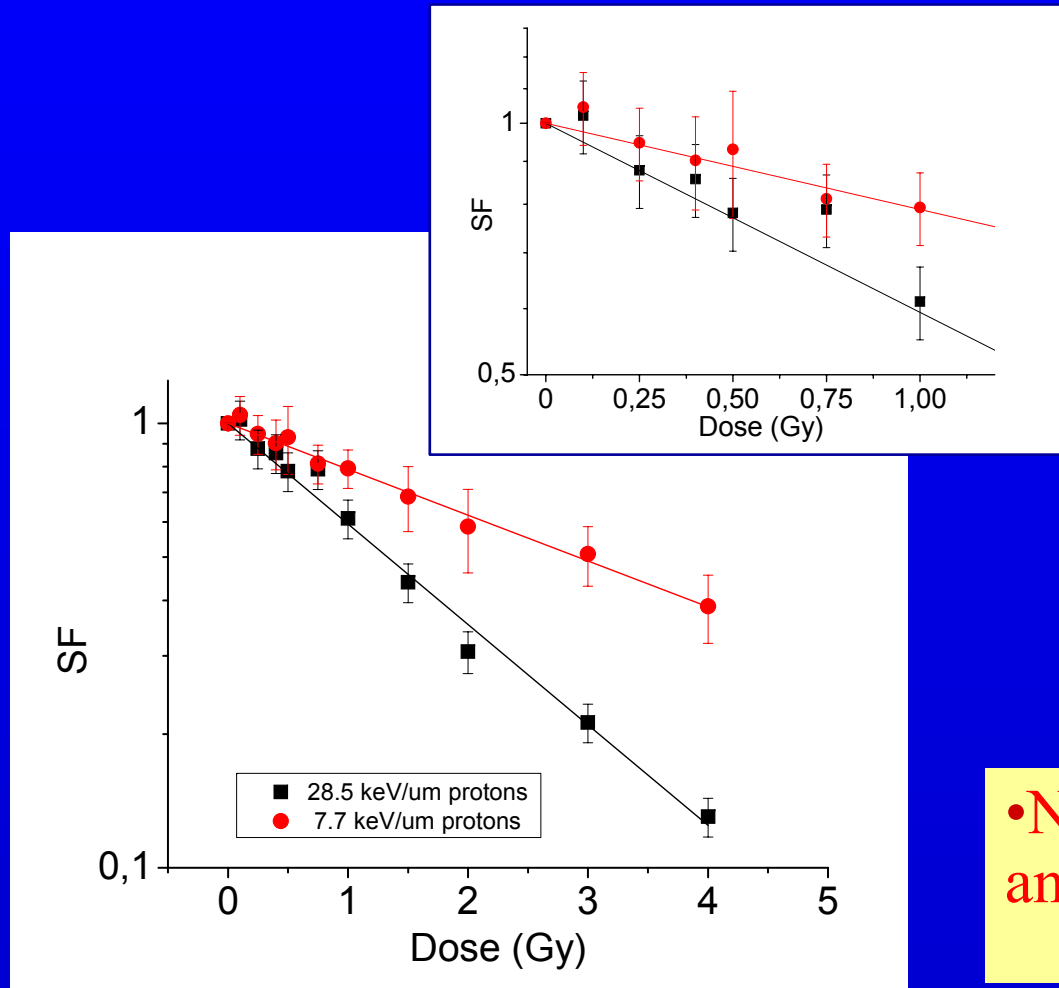


LNL broad ion beam cell irradiations:

- ^{60}Co γ -rays and $^4\text{He}^{2+}$ ions of different energies (59, 79 and 102 keV/ μm LET)
 - Chinese hamster V79 cells
- ↓
- Low dose hyper-radiosensitivity
 - Induced radioresistance

Hyper-radiosensitivity and Induced radioresistance

(Cherubini et al., Rad. Prot. Dos. 143, 2011)



LNL broad ion beam
cell irradiations :

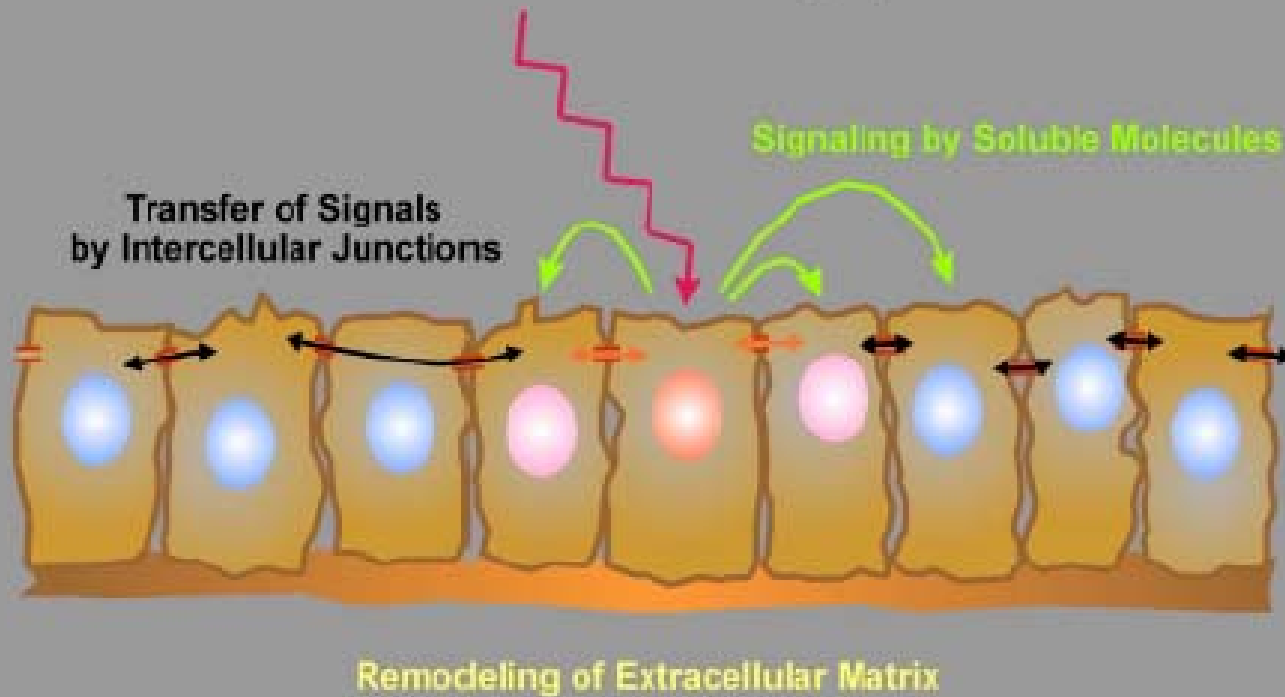
- Protons ($^1\text{H}^+$)
(LET: 7.7, 28.5 keV/ μm)
- Chinese Hamster V79 cells



• No Hyper-radiosensitivity
and Induced Radioresistance

Bystander Effect Mechanisms

Radiation-Induced Cell Stress / Injury

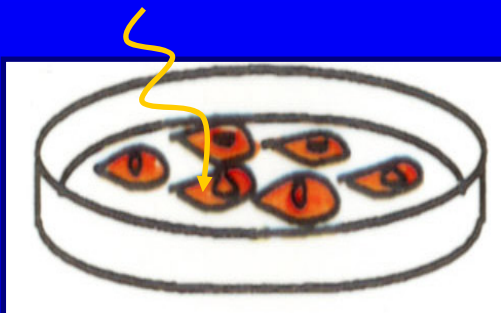


G. Nelson, 2000

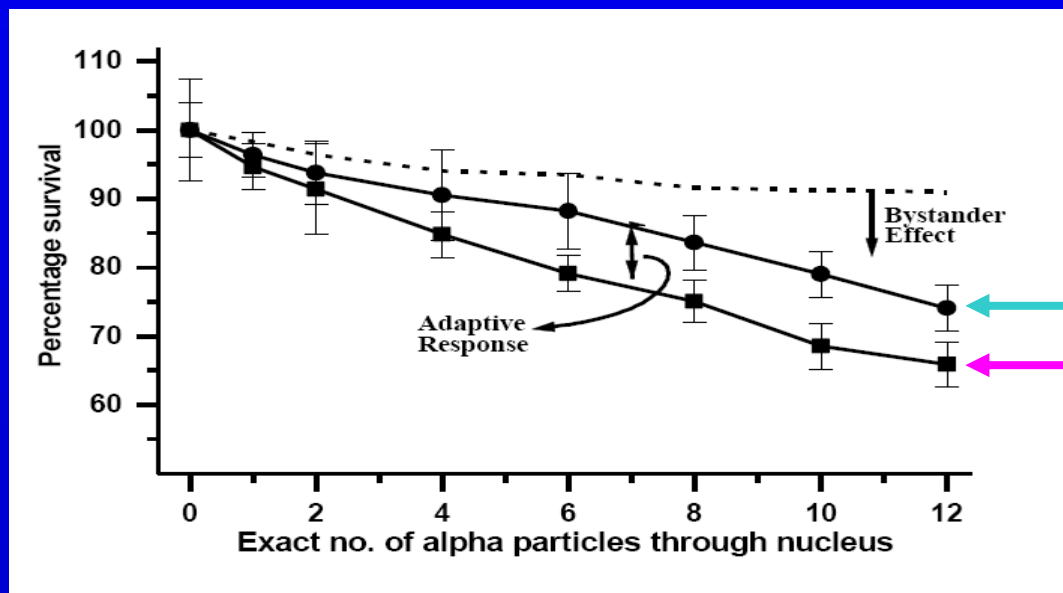
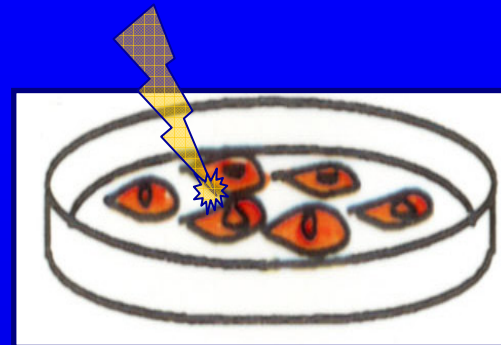
Una cellula colpita all'interno di una popolazione *in-vitro*
→ Danno riscontrato in più di una cellula

Adaptive Response

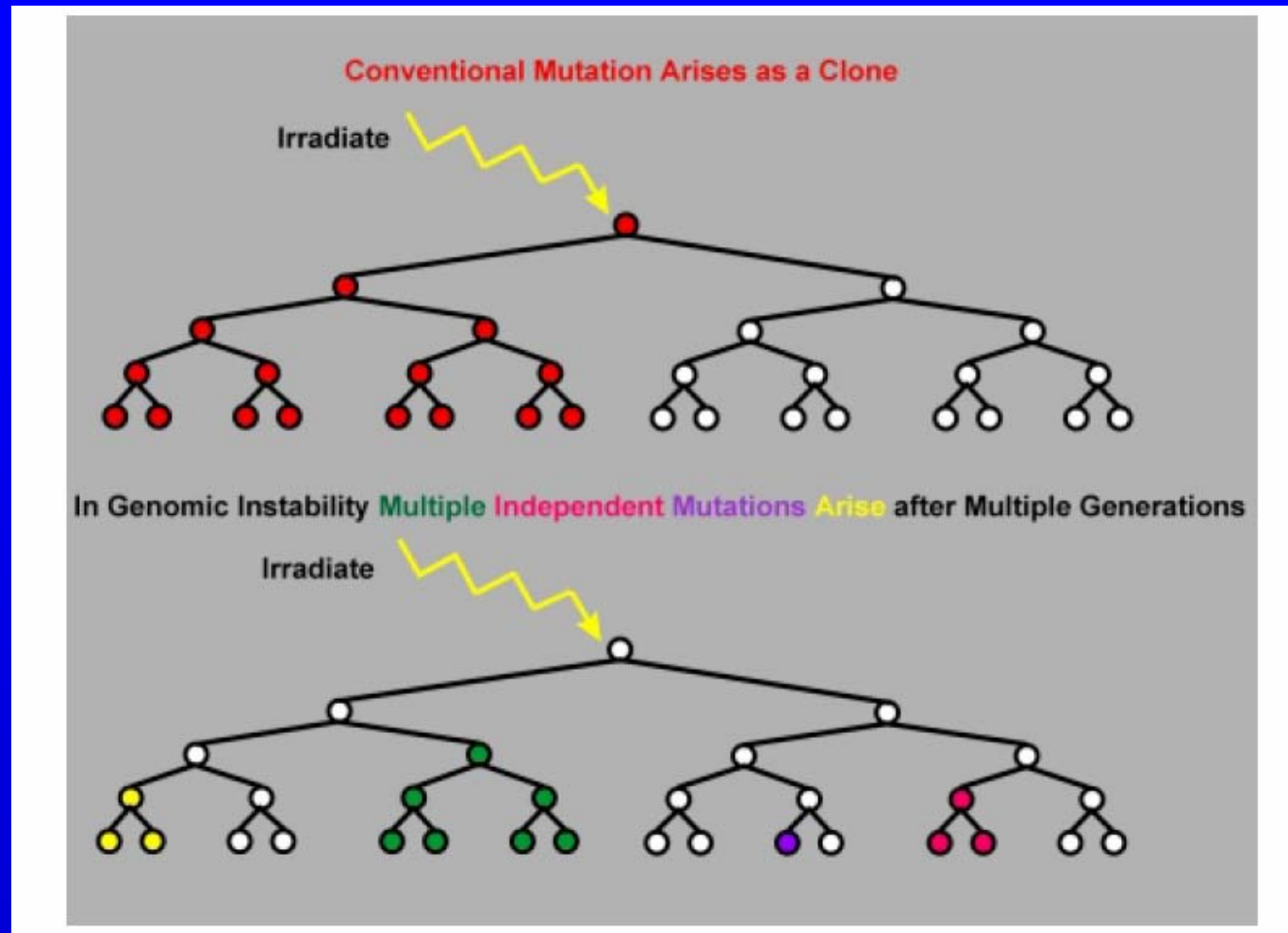
1) Priming dose: 5-40 cGy RX



2) Challenging dose



...Genomic Instability...



Nelson, 2000

...Kadhim et al. (1992), Limoli et al. (1999, 2000)....

...But also....

Lack of Bystander Effects from High-LET Radiation for Early Cytogenetic End Points

Torsten Groesser,¹ Brian Cooper and Bjorn Rydberg

Lawrence Berkeley National Lab

Lawrence Berkeley National Lab, Radiation Physics Division, Department of Genome Stability, Berkeley, California

RADIATION RESEARCH 171, 530–540 (2009)
0033-7587/09 \$15.00
© 2009 by Radiation Research Society.
All rights of reproduction in any form reserved.

No Evidence for DNA and Early Cytogenetic Damage in Bystander Cells after Heavy-Ion Microirradiation at Two Facilities

C. Fournier,^{a,1} P. Barberet,^a T. Pouthier,^a S. Ritter,^a B. Fischer,^a K. O. Voss,^a T. Funayama,^b N. Hamada,^{b,c} Y. Kobayashi^{b,c} and G. Taucher-Scholz^a

^a Department of Biophysics, Gesellschaft für Schwerionenforschung, 64291 Darmstadt, Germany; ^b Microbeam Radiation Biology Group, National Institute of Advanced Industrial Science and Technology, Tsukuba, Ibaraki, Gunma 370-1292, Japan; and ^c Department of Radiation Oncology, School of Medicine, Maebashi, Gunma 371-8511, Japan

Int. J. Radiat. Biol., Vol. 86, No. 2, February 2010, pp. 102–113

informa
healthcare

Lack of evidence for low-LET radiation induced bystander response in normal human fibroblasts and colon carcinoma cells

MARIANNE B. SOWA¹, WILFRIED GOETZ², JANET E. BAULCH², DINAH N. PYLES², JAROSLAW DZIEGIELEWSKI³, SUSANNAH YOVINO², ANDREW R. SNYDER⁴, SONIA M. DE TOLEDO⁵, EDOUARD I. AZZAM⁵, & WILLIAM F. MORGAN^{1,2}

¹Molecular and Cellular Biology, Pacific Northwest Research Laboratory and Greenebaum Cancer Center, National Cancer Institute, Bethesda, Maryland, USA
²Radiation Oncology, University of Virginia, Charlottesville, Virginia, USA
³Department of Radiology, University of Medicine and Dentistry of New Jersey, Newark, New Jersey, USA
⁴Department of Radiology, University of Medicine and Dentistry of New Jersey, Newark, New Jersey, USA
⁵Department of Radiology, University of Medicine and Dentistry of New Jersey, Newark, New Jersey, USA

Radiation Protection Dosimetry (2010), Vol. 0, No. 0, pp. 0–0
DOI: 10.1093/rpd/nc0000

RPD 143, 2011

SECTION TITLE HERE

LACK OF HYPER-RADIOSENSITIVITY AND INDUCED RADIORESISTANCE AND OF BYSTANDER EFFECT IN V79 CELLS AFTER PROTON IRRADIATION OF DIFFERENT ENERGIES

R. Cherubini¹, V. De Nadal¹, S. Gerardi^{1,*}, D. Guryev^{1,2}
¹Istituto Nazionale di Fisica Nucleare – Laboratori Nazionali di Legnaro, Viale dell'Università 2, 35020 Legnaro, Padova, Italy
²Russian Academy of Sciences – Komi Science Centre, Syktyvkar, Russia

Istituto Nazionale di Fisica Nucleare – Legnaro, 19 Aprile 2013

Ri-Definizione del *target* della radiazione ..???

- **Target extra-nucleari:** citoplasma ... oltre al nucleo ...
- **Target extra-cellulari:** cellule non direttamente irraggiate ...oltre a quelle irraggiate ...



Il DNA ha perso il ruolo di *target* della radiazione?

Quali sono i meccanismi di induzione e trasmissione del danno?



Implicazioni in radioprotezione per le valutazioni di rischio alle basse dosi?

Implicazioni in adroterapia per le valutazioni di rischio per i tessuti sani circostanti il volume tumorale irraggiato?

...problemi aperti...

Aug 1, 2003

How particles can be therapeutic

Note added 2 December 2003. This article received a Special Commendation in the General Medical category of the [Medical Journalism Awards 2003](#).

Subatomic particles are proving highly effective in treating cancer, as Matthew Chalmers reports. The goal today is to get them out of physics labs and into hospitals

Until a cure for cancer is found, about one in three of us will probably have to undergo surgery, chemotherapy or radiotherapy at some point in our lives. Traditional radiotherapy uses X-rays to target cancerous tissue, but there is growing interest in using particles instead. Beams of hadrons, such as protons, neutrons and ions, offer important advantages over X-ray radiotherapy. Their clinical applications, however, are much less widespread.

Most of the 25 or so hadron-therapy facilities that are currently in operation around the world are sited at large particle-physics laboratories - not hospitals. A major focus of the hadron-therapy session at the World Congress in Medical Physics and Bioengineering, which is taking place in Sydney this month, will be on efforts to transform particle therapy into a practical and affordable treatment option.

Particle therapy works by damaging the DNA of cancerous cells - mostly by ionization - so that they cannot grow and multiply, while minimizing damage to surrounding healthy tissue. This is the same basic principle behind X-ray therapy (see "[X-rays pinpoint tumour targets](#)"). However, photons lose a significant amount of their energy before they reach the tumour, which can damage healthy cells and cause unpleasant side effects.

On the other hand, when a beam of charged particles enters the body, it deposits most of its energy at a depth that depends precisely on the energy of the particles. This means that tumours can be targeted more accurately, allowing a larger radiation dose to be delivered and speeding up the treatment programme.

Proton therapy

The most widely used form of particle therapy is proton therapy, which was proposed by Robert Wilson - the first director of Fermilab in the US - in 1946. The first proton therapy was carried out in 1954 with the Bevatron accelerator at Berkeley, and to date about 35,000 patients around the world have undergone the treatment, mostly for cancers of the retina. Over 9000 of these were treated over the course of 30 years at the Harvard Cyclotron Laboratory in Massachusetts. The programme was transferred to the Massachusetts General Hospital in Boston last year, making it the world's second hospital-based proton-therapy centre.

physicsworld.com; Aug. 1, 2003

Heavy treatment

Newer than protons on the particle-therapy scene is ion therapy. Heavy ions, such as carbon, have a higher RBE than protons and are thought to provide more effective treatment for certain, deep-seated tumours that are often "radioresistant".

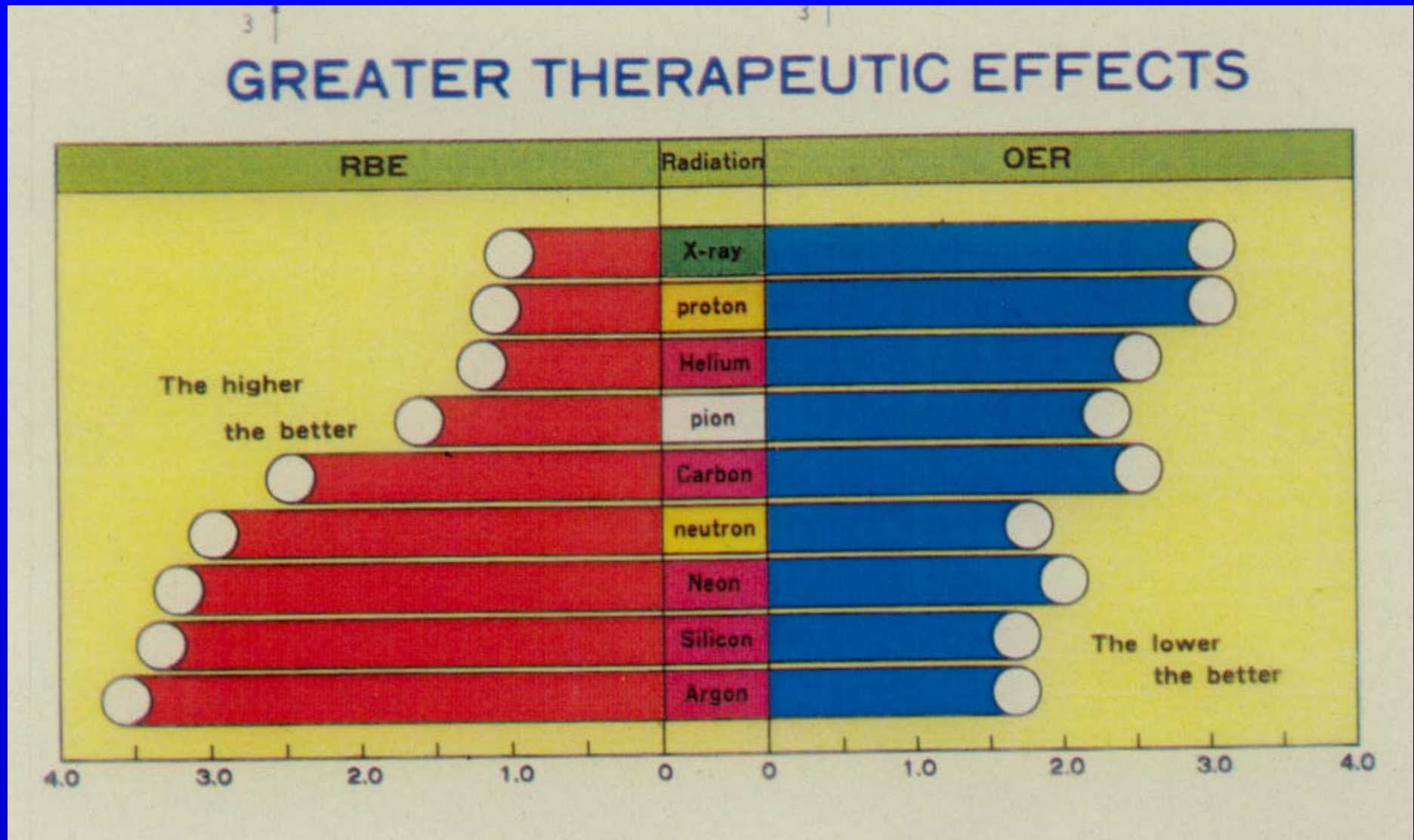
This is because the rate at which a charged particle loses energy in a material - which is quantified by its linear energy transfer (LET) - increases with the mass of the particle. Helium ions were used to treat over 2000 patients at the Bevelac accelerator at Berkeley from 1957 and 1992, while neon ions have been used to treat a further 430. However, the optimal RBE using ions has since been found to lie in the range between lithium and carbon. There are currently just three heavy-ion treatment facilities in the world - two in Japan and one in Germany - all of which use carbon ions.

physicsworld.com; Aug. 1, 2003

....Advantages offered by Accelerated Charged particles for tumor treatment (Hadrontherapy)

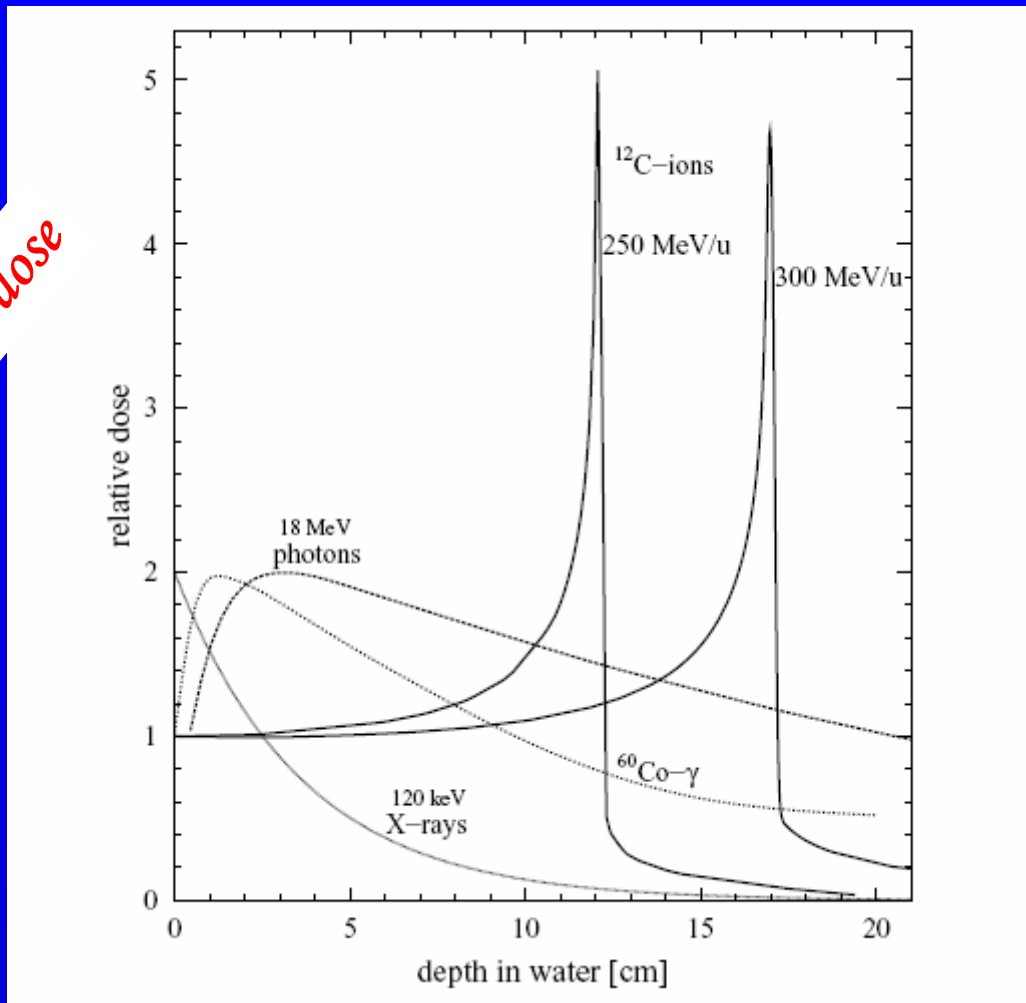
- Small values of range and straggling
- Inverse depth-dose profile (Bragg peak at the target volume)
- High values of RBE (Relative Biological Effectiveness)
- Small values of OER (Oxygen Enhancement Ratio)
- Reduced dependence on the cell radiosensitivity (and on the cell cycle)
- Possibility for a on-line depth-dose profile monitoring by the in-beam PET (Positron Emission Tomography)

...hadrontherapy application....

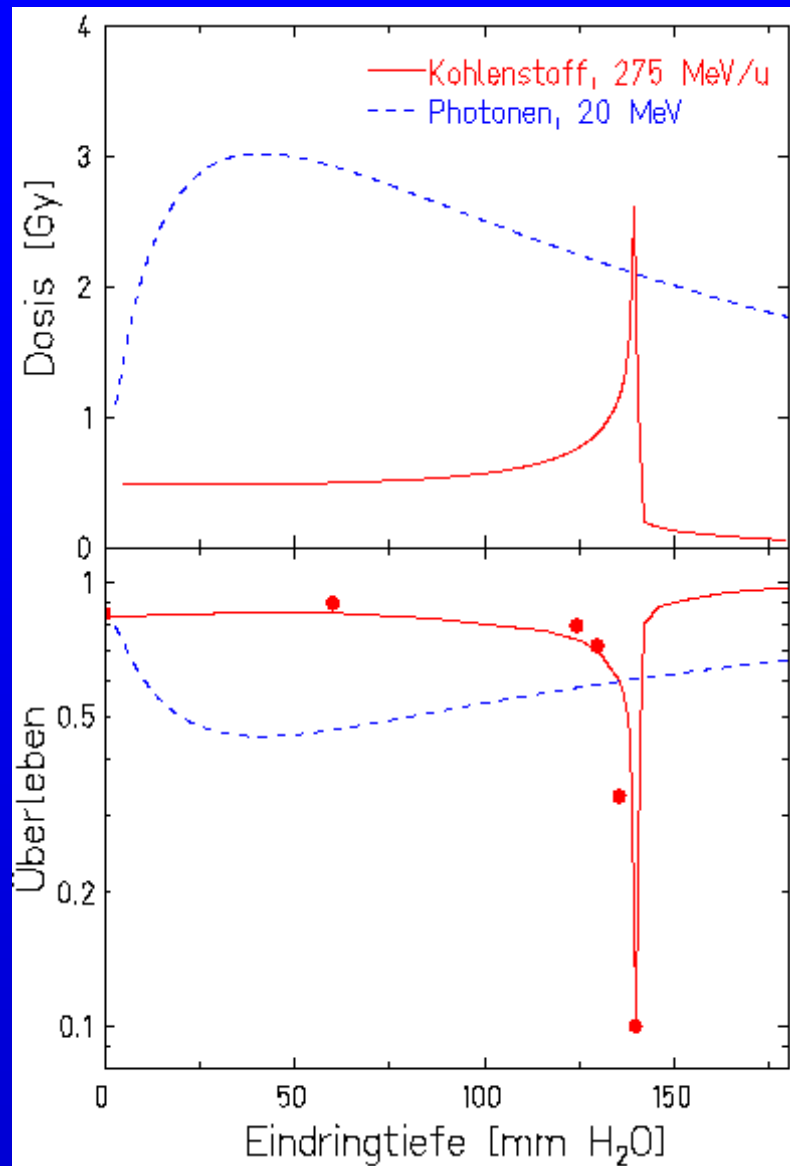


...depth dose profiles of X-rays, ^{60}Co -gamma and Röntgen-Bremsstrahlung with Carbon ions of 250 MeV/u and 300 MeV/u

→ Localizzazione della dose



(G. Kraft, GSI)



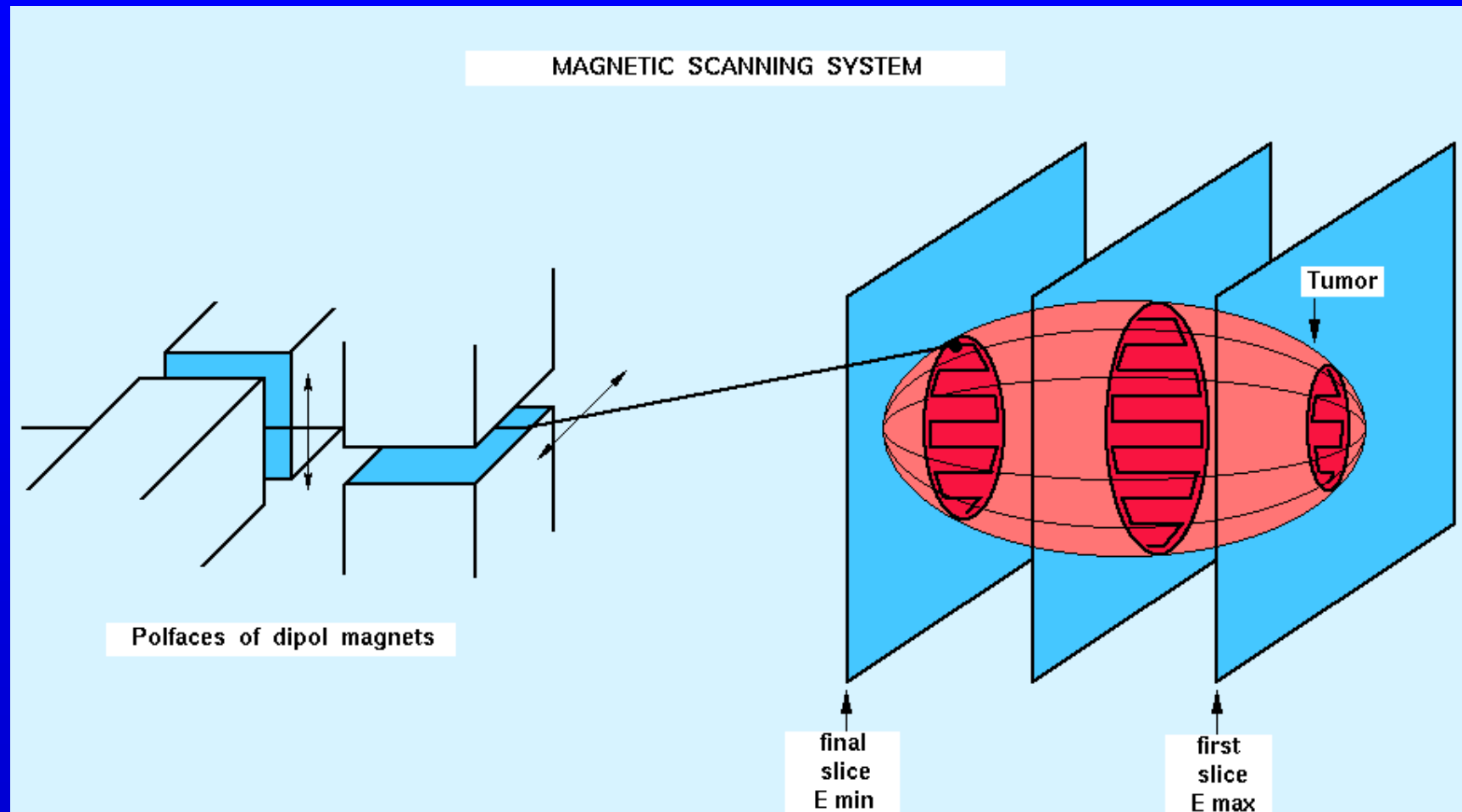
Comparison of the physical dose distribution (upper diagram) and the survival rate of cells (lower diagram) as a function of penetration depth for ion and photon beams.

The enhanced energy deposition at the end of the particle range and the corresponding dramatic decrease of cell survival show that heavy ion beams are excellent tools for the treatment of deep seated tumours.

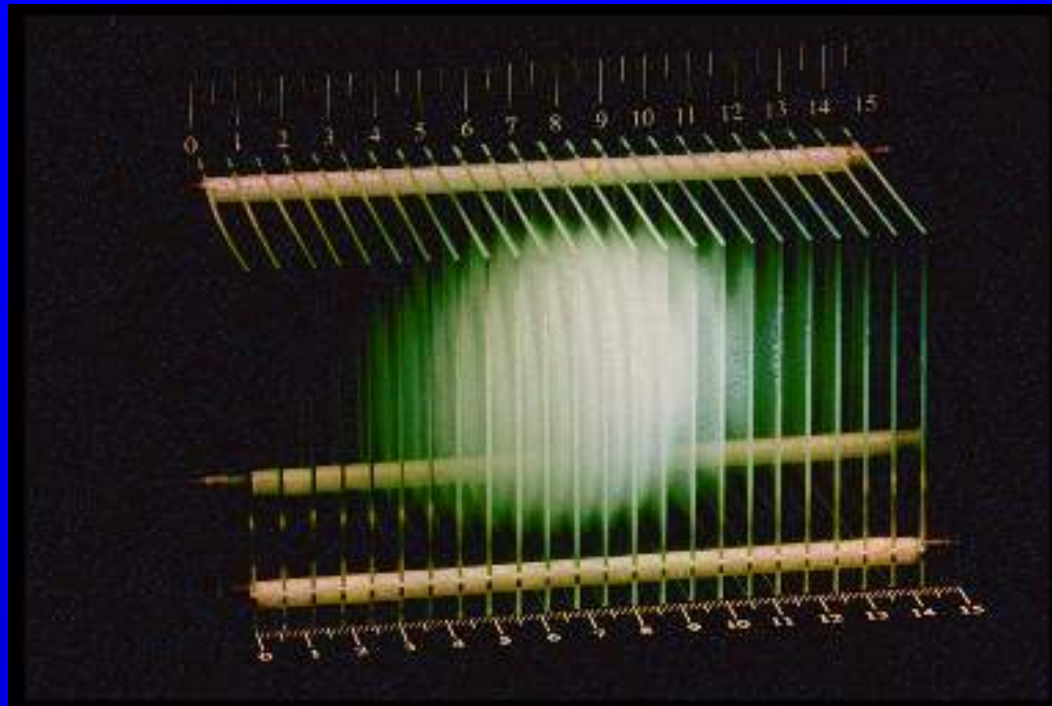
(Kraft et al, GSI)

Tumour Painting

Conformal irradiation



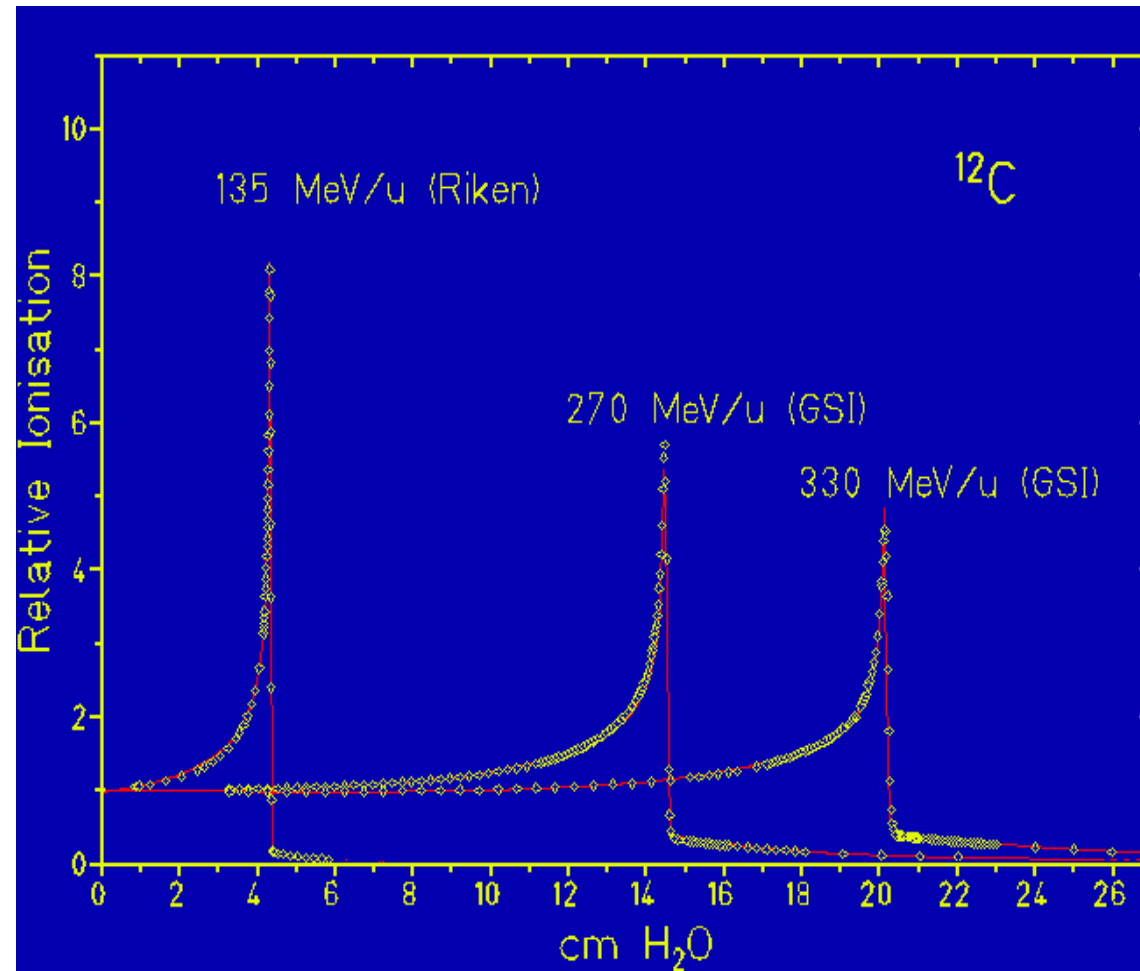
GSI, Darmstadt



GSI, Darmstadt

A spherical volume of 6 cm diameter between 9 and 15 cm depth in water was irradiated with carbon ions of 270 MeV per nucleon. CR-39 nuclear track detectors were placed in water in steps of a few mm. After etching they show the precise delivery of dose in the target volume.

Measured depth dose distributions (Bragg curves) in water (points) compared with GSI model calculations (red curves).



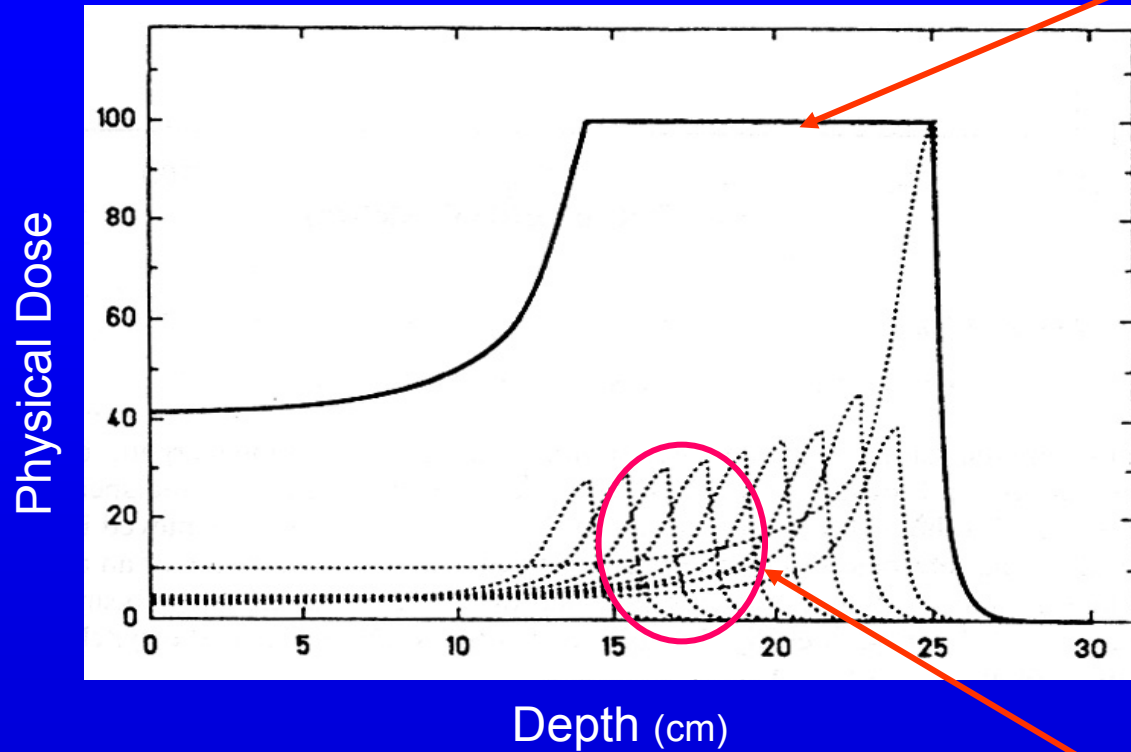
www.gsi.de

When heavy ions pass through a thick absorber like the human body even small cross sections for nuclear reactions produce a significant amount of lighter reaction products.

In radiotherapy the change in *biological effectiveness* between the primary ions and the *lighter secondaries* has to be taken into account in *treatment planning*, as well as their longer range.

SOBP: Spread Out Bragg Peak

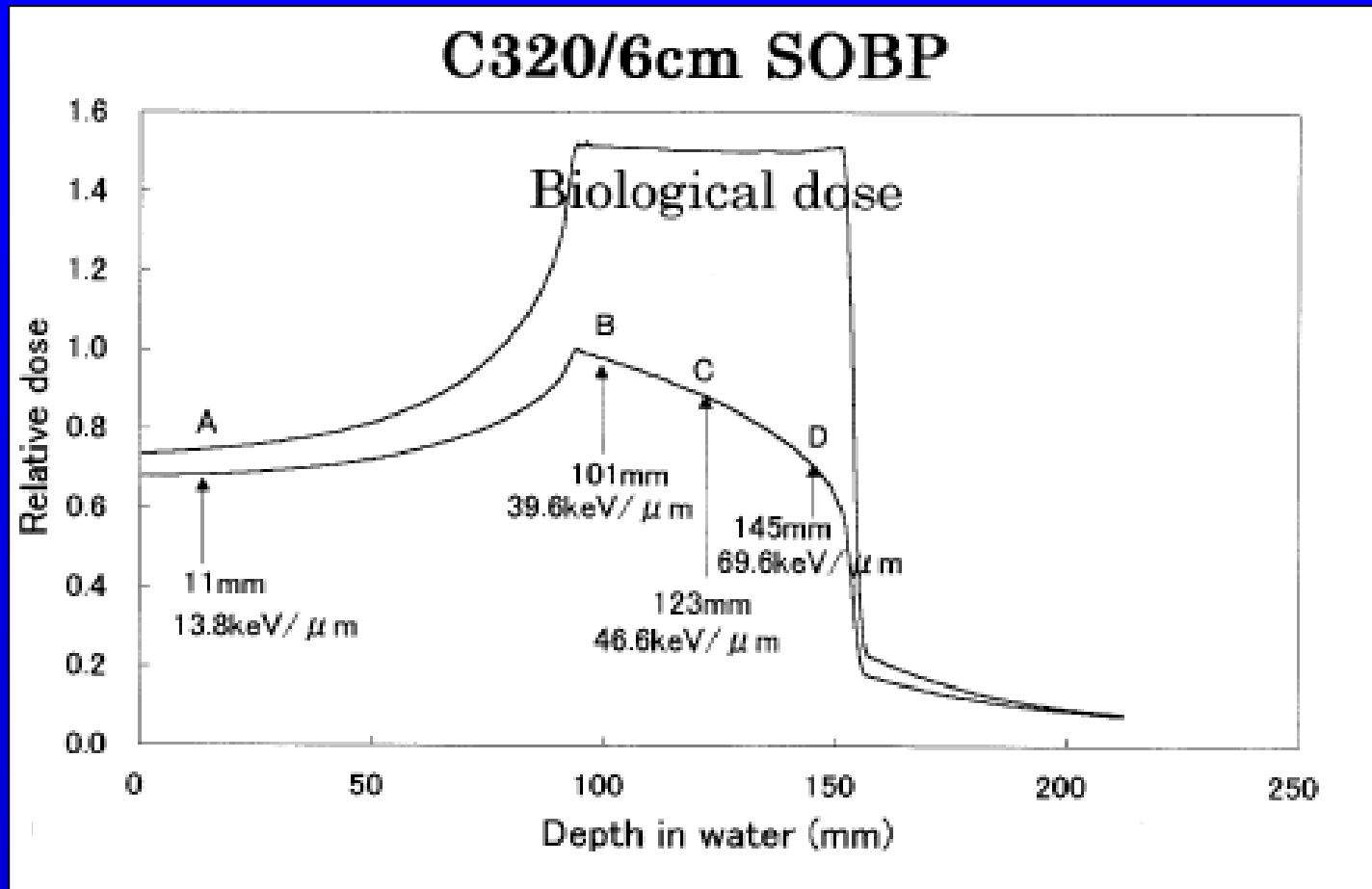
SOBP
Spread Out Bragg Peak



*Contributions from primary ions of various energies
...and, for light-ions (i.e. C12), from various lighter ions
(primary ion beam fragmentation)*

Physical dose → Biological dose

$$D_{\text{Biol}}(x = x_i) = D_{\text{Phys}}(x = x_i) \times \text{RBE}(x = x_i), \quad i = 1 \dots n$$



(Kagawa 2002 - HIBMC di Hyogo, Japan)

Physical dose → Biological dose

$$D_{\text{Biol}}(x = x_j) = D_{\text{Phys}}(x = x_j) \times \text{RBE}(x = x_j), \quad i = 1 \dots n$$

Heavy-ion radiotherapy planning: biological dose

3329

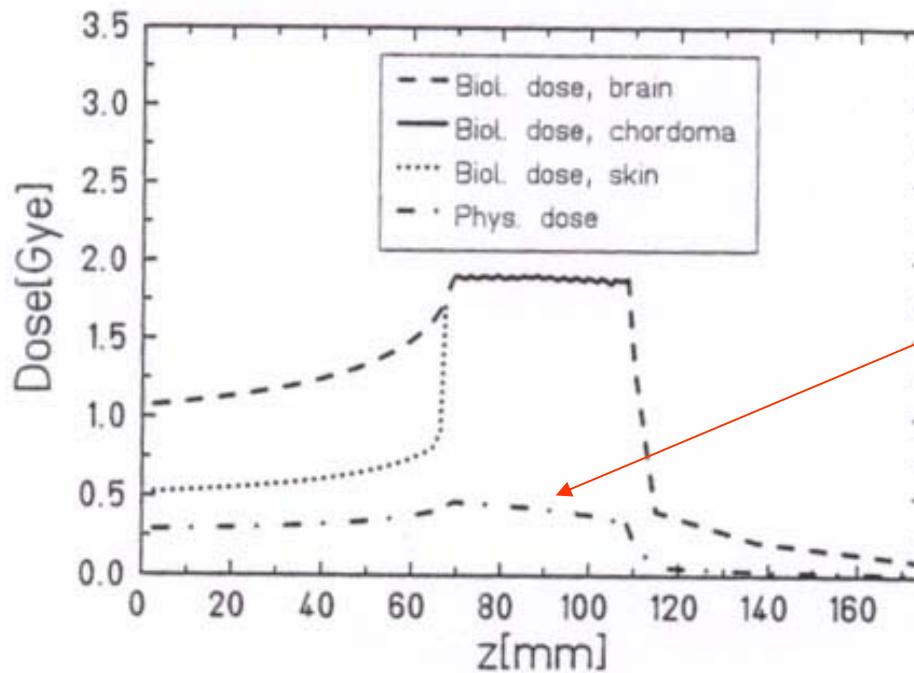
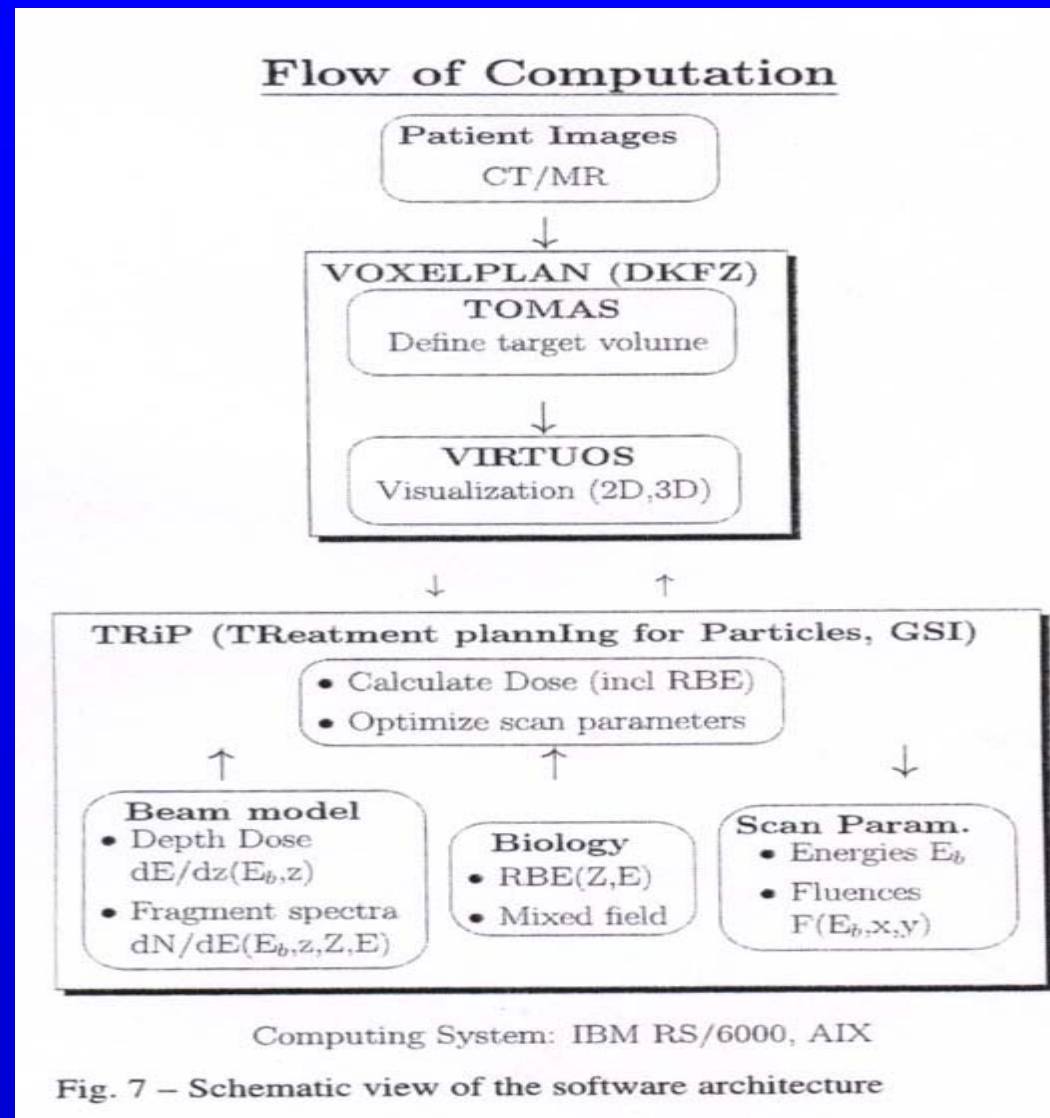
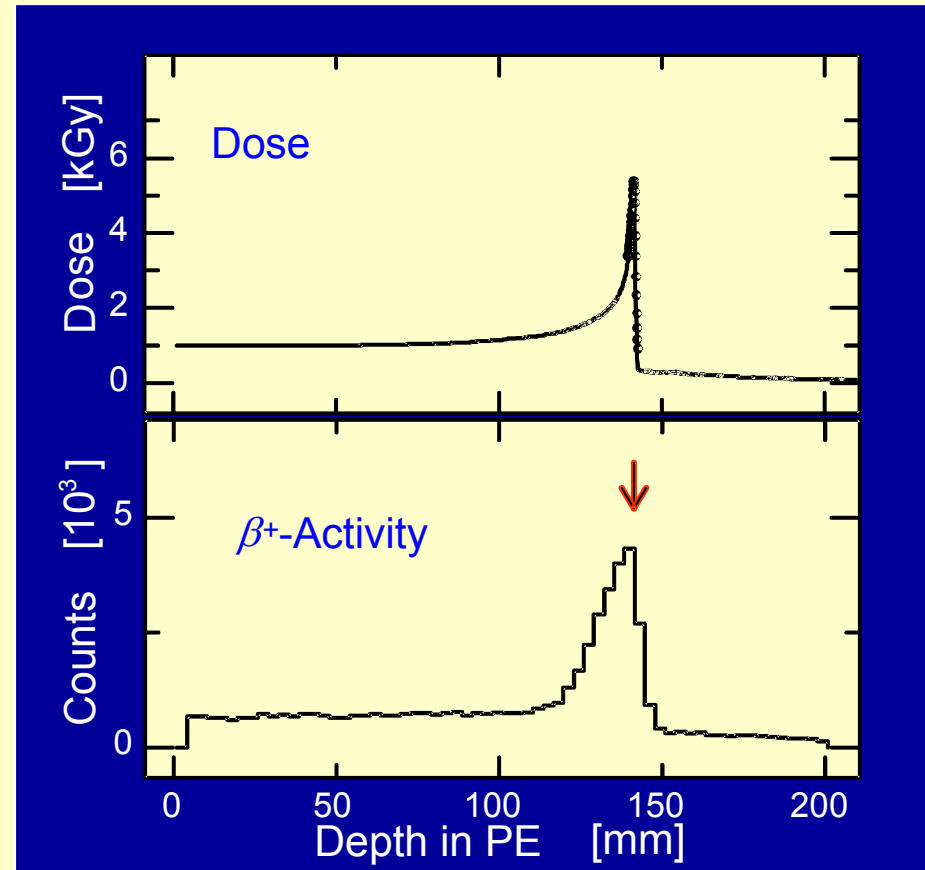
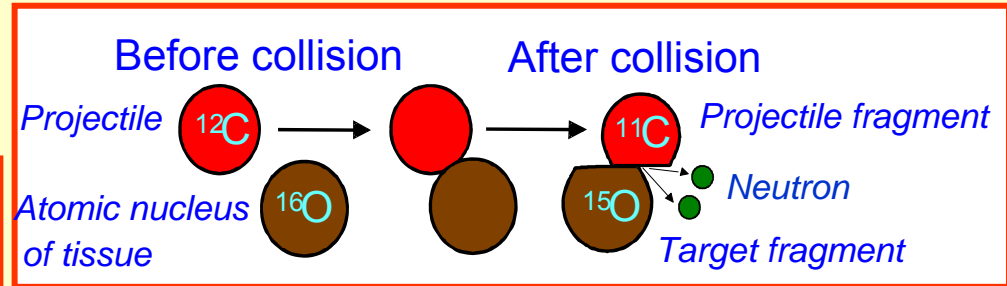
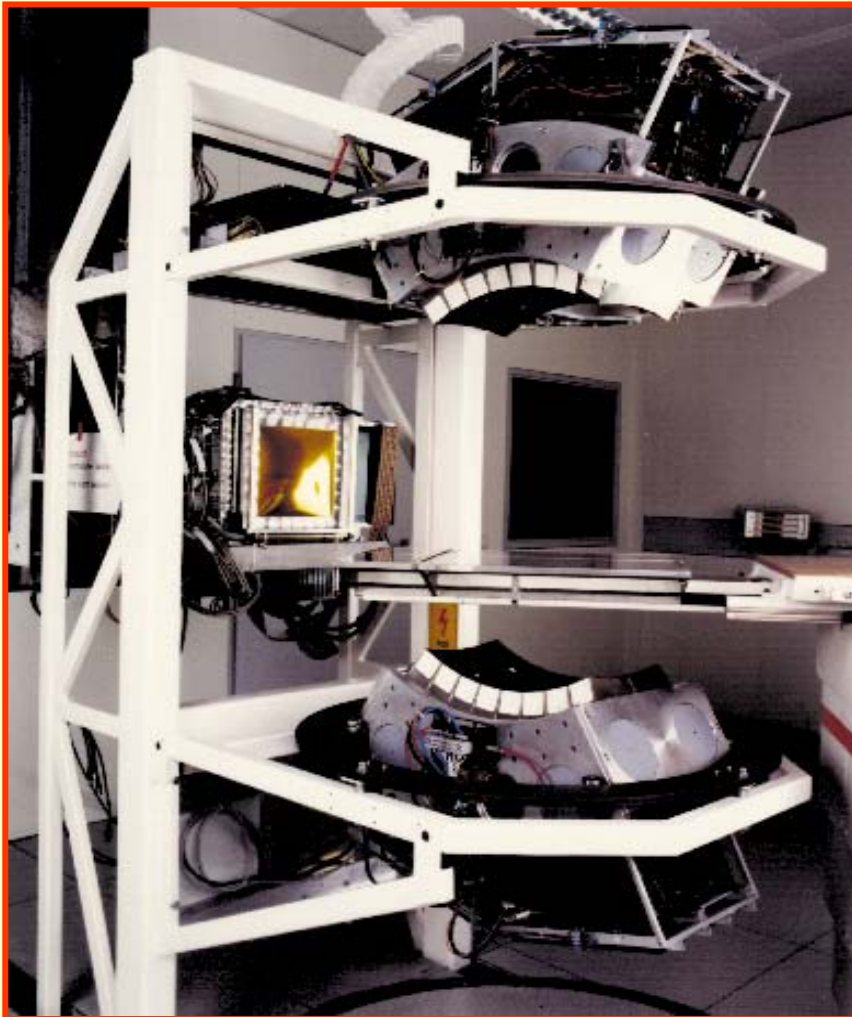


Figure 6. Biologically effective depth dose distributions calculated for different tissue types on a line through the isocentre in a water-equivalent system (beam enters from the left hand side).

GSI treatment planning package TRiP98



"Useful fragments"... In-beam PET



Hadron Therapy Patient Statistics (data received from centers per end of March 2013)

Hadron Therapy Patient Statistics (data received from centers per end of March 2013)

Patient Statistics (for the facilities out of operation):

WHERE		PARTICLE	FIRST PATIENT	PATIENT TOTAL	LAST PATIENT	
Belgium	Louvain-la-Neuve	p	1991	21	1993	ocular tumors only
Canada	Vancouver (TRIUMF)	π^-	1979	367	1994	ocular tumors only
Germany	Darmstadt (GSI)	C-ion	1997	440	2009	
Japan	Tsukuba (PMRC, 1)	p	1983	700	2000	
Japan	Chiba	p	1979	145	2002	ocular tumors only
Japan	WERC	p	2002	62	2009	
Russia	Dubna (1)	p	1967	124	1996	
Sweden	Uppsala (1)	p	1957	73	1976	
Switzerland	Villigen PSI (SIN-Piotron)	π^-	1980	503	1993	
Switzerland	Villigen PSI (OPTIS 1)	p	1984	5458	2010	ocular tumors only
CA., USA	Berkeley 184	p	1954	30	1957	
CA., USA	Berkeley	He	1957	2054	1992	
CA., USA	Berkeley	ion	1975	433	1992	
IN., USA	Bloomington (MPRI, 1)	p	1993	34	1999	ocular tumors only
MA., USA	Harvard	p	1961	9116	2002	
NM., USA	Los Alamos	π^-	1974	230	1982	

19790 Total

thereof

2054 He
1100 pions
440 C-ions
433 other ions
15763 protons

Hadron Therapy Patient Statistics (data received from centers per end of March 2013)

March 2013 - Martin Jermann, PTCOG Secretary

Italy

Patient Statistics (for facilities in operation end of 2012):

WHERE		PARTICLE	FIRST PATIENT	PATIENT TOTAL	DATE OF TOTAL	
Canada	Vancouver (TRIUMF)	p	1995	170	Dec-12	ocular tumors only
Czech Rep.	Prag (PTCCZ)	p	2012	1	Dec-12	
China	Wanjie (WPTC)	p	2004	1078	Dec-12	
China	Lanzhou	C ion	2006	194	Dec-12	
England	Clatterbridge	p	1989	2297	Dec-12	ocular tumors only
France	Nice (CAL)	p	1991	4692	Dec-12	ocular tumors only
France	Orsay (CPO)	p	1991	5949	Dec-12	4748 ocular tumors
Germany	Berlin (HMI)	p	1998	2084	Dec-12	ocular tumors only
Germany	Munich (RPTC)	p	2009	1377	Dec-12	
Germany	HIT, Heidelberg	C ion	2010	980	Dec-12	
Germany	HIT, Heidelberg	p	2010	252	Dec-12	
Italy	Catania (INFN-LNS)	p	2002	293	Nov-12	ocular tumors only
Italy	Pavia (CNAO)	p	2011	42	Dec-12	
Italy	Pavia (CNAO)	C ion	2012	3	Dec-12	
Japan	Chiba (HIMAC)	C ion	1994	7331	Jan-13	72 with scanning
Japan	Kashiwa (NCC)	p	1998	1226	Mar-13	
Japan	Hyogo (HIBMC)	p	2001	3198	Dec-11	
Japan	Hyogo (HIBMC)	C ion	2002	1271	Dec-11	
Japan	Tsukuba (PMRC, 2)	p	2001	2516	Dec-12	
Japan	Shizuoka	p	2003	1365	Dec-12	
Japan	Koriyama-City	p	2008	1812	Dec-12	
Japan	Gunma	C ion	2010	537	Dec-12	
Japan	Ibusuki (MMRI)	p	2011	490	Dec-12	
Korea	Ilsan, Seoul	p	2007	1041	Dec-12	
Poland	Krakow	p	2011	15	Dec-12	ocular tumors only
Russia	Moscow (ITEP)	p	1969	4300	Dec-12	estimated
Russia	St. Petersburg	p	1975	1386	Dec-12	
Russia	Dubna (JINR, 2)	p	1999	922	Dec-12	
South Africa	iThemba LABS	p	1993	521	Dec-11	
Sweden	Uppsala (2)	p	1989	1267	Dec-12	
Switzerland	Villigen-PSI, incl OPTIS2	p	1996	1409	Dec-12	498 ocular tumors
USA, CA.	UCSF - CNL	p	1994	1515	Dec-12	ocular tumors only
USA, CA.	Loma Linda (LLUMC)	p	1990	16884	Dec-12	
USA, IN.	Bloomington (IU Health PTC)	p	2004	1688	Dec-12	
USA, MA.	Boston (NPTC)	p	2001	6550	Oct-12	
USA, TX.	Houston (MD Anderson)	p	2006	3909	Dec-12	
USA, FL	Jacksonville (UFPTI)	p	2006	4272	Dec-12	
USA, OK.	Oklahoma City (ProCure PTC)	p	2009	1045	Dec-12	
USA, PA.	Philadelphia (UPenn)	p	2010	1100	Dec-12	
USA, NY.	New Jersey ProCure PTC)	p	2012	137	Dec-12	
USA, IL.	CDH Warrenville	p	2010	840	Dec-12	
USA, VA.	Hampton (HUPTI)	p	2010	489	Dec-12	

88448 Total

thereof 10316 C-ions
78132 protons

Total for all facilities (in operation and out of operation):
2054 He
1100 pions
10756 C-ions
433 other ions
93895 protons
108238 Grand Total

http://ptcog.web.psi.ch/Archive/pat_statistics/Patientstatistics-updateMar2013.pdf

Particle therapy facilities in a planning stage or under construction:

WHO, WHERE	COUNTRY	PARTICLE	MAX. CLINICAL ENERGY (MeV)	BEAM DIRECTION	NO. OF TREATMENT ROOMS	START OF TREATMENT PLANNED
Med-AUSTRON, Wiener Neustadt*	Austria	p, C-ion	430/u synchrotron	1 gantry (only for protons) 1 fixed beam, 1 fixed 0 + 90 deg	3	2015
ATreP, Trento*	Italy	p	230 cyclotron	2 gantries 1 horiz fixed beam	3	2013
Fudan University Shanghai CC*	China	p, C-ion	430/u synchrotron	3 fixed beams	3	2014
McLaren PTC, Flint, Michigan*	USA	p	250/330 synchrotron	3 gantries	3	2013
WPE, Essen*	Germany	p	230 cyclotron	3 gantries, 1 horiz fixed beam	4	2013
HITFil, Lanzhou*	China	C-ion	400/u synchrotron	4 horiz, vertical, oblique, fixed beams	4	2013
PTC, Marburg*	Germany	p, C-ion	430/u synchrotron	3 horiz fixed beams 1 fixed beam 0 + 45 deg	4	2013?
Northern Illinois PT Res.Institute, W. Chicago, IL*	USA	p	250 SC cyclotron	2 gantries, 2 horiz fixed beams	4	2013?
Chang Gung Memorial Hospital, Taipei*	Taiwan	p	235 cyclotron	4 gantries, 1 experimental room	4	2013?
SAGA, HIMAT, Tosu-Shi*	Japan	C-ion	400/u synchrotron	3 horiz/vertical fixed beams	3	2013
Fukui Prefectural Hospital PTC, Fukui City*	Japan	p	230 ?	?	?	2014?
PMHPTC, Protvino*	Russia	p	250 synchrotron	1 horiz fixed beam	1	2013?

* under construction

CCSR, Bratislava	Slovak Rep.	p	72 cyclotron	1 horiz fixed beam	1	?
CMHPTC, Ruzomberok*	Slovak Rep.	p	250 synchrotron	1 horiz fixed beam	1	?
SJFH, Beijing	China	p	230 cyclotron	1 gantry, 1 horiz fixed beam	2	?
Skandion Clinic, Uppsala*	Sweden	p	230 cyclotron	2 gantries	2	2013
Barnes Jewish St. Louis, MO*	USA	p	250 SC synchro-cyclotron	1 gantry	1	2013
Scripps Proton Therapy Center, San Diego, CA*	USA	p	250 SC cyclotron	3 gantries, 2 horiz fixed beams	5	2013
Samsung Proton Center, Seoul*	South Korea	p	230 cyclotron	2 gantries	2	2014
Robert Wood Johnson, New Brunswick*	USA	p	250 SC synchro-cyclotron	1 gantry	1	2013
Oklahoma University, Oklahoma City, OK*	USA	p	250 SC synchro-cyclotron	1 gantry	1	2013
MD Anderson, Orlando, FL*	USA	p	250 SC synchro-cyclotron	1 gantry	1	2013
First Coast Oncology, Jacksonville, FLI*	USA	p	250 SC synchro-cyclotron	1 gantry	1	2013
Centre Antoine Lacassagne, Nice*	France	p	230 SC synchro-cyclotron	1 gantry	1	2014
IFJ PAN, Krakow*	Poland	p	235 cyclotron	1 gantry	1	2014?
PTC Zürichobersee, Galgenen	Switzerland	p	230 cyclotron	4 gantries, 1 horiz fixed beam	5	2016

....Grazie....



RBE for carbon track-segment irradiation in cell lines of differing repair capacity

W. K. WEYRATHER†*, S. RITTER†, M. SCHOLZ†‡ and G. KRAFT†

(Received 7 April 1999; accepted 5 July 1999)

Abstract.

Purpose: The LET position of the RBE maximum and its dependence on the cellular repair capacity was determined for carbon ions. Hamster cell lines of differing repair capacity were irradiated with monoenergetic carbon ions. RBE values for cell inactivation at different survival levels were determined and the differences in the RBE-LET patterns were compared with the individual sensitivity to photon irradiation of the different cell lines.

Material and methods: Three hamster cell lines, the wild-type cell lines V79 and CHO-K1 and the radiosensitive CHO mutant *xrs5*, were irradiated with carbon ions of different energies (2.4–266.4 MeV/u) and LET values (13.7–482.7 keV/μm) and inactivation data were measured in comparison to 250 kV x-rays.

Results: For the repair-proficient cell lines a RBE maximum was found at LET values between 150 and 200 keV/μm. For the repair-deficient cell line the RBE failed to show a maximum and decreased continuously for LET values above 100 keV/μm.

Conclusions: The carbon RBE-LET relationship for inactivation is shifted to higher LET values compared with protons and α-particles. RBE correlated with the repair capacity of the cells.

1. Introduction

Carbon ions are of special interest for radiation therapy due to their particular physical and radiobiological properties, i.e. the physical selectivity and the increased relative biological effectiveness (RBE). For the calculation of the biological response in an extended volume like a tumor, RBE values have to be known for all LET values used and all relevant survival levels. Since Barendsen (Barendsen *et al.* 1963) measured the dependence of RBE upon LET for helium ions, the RBE-LET relationship has been measured for many cell types and radiations (Todd 1967, Hall *et al.* 1977, Blakely *et al.* 1979, Tobias *et al.* 1984, Wulf *et al.* 1985, Kraft 1987, Belli *et al.* 1989, Folkard *et al.* 1996, Suzuki *et al.* 1997). However, it is difficult to compare measurements performed at institutions using passive energy variation. From energy variation produced by absorbers a large number of lighter fragments is generated which yields

*Author for correspondence;
e-mail: W.Kraft-Weyrather@gsi.de

†Gesellschaft für Schwerionenforschung, Planckstr. 1,
D-64291 Darmstadt, Germany.

‡Radiologische Klinik, Im Neuenheimer Feld 400, D-69120,
Heidelberg, Germany.

a different LET composition from an active energy variation by the accelerator. Nevertheless some common conclusions can be drawn from these measurements:

1. The RBE-LET relation does not form a common line for all types of radiation, but has separate peaks for different atomic numbers, that shift to higher LET values for heavier ions (e.g. Kraft 1987).
2. RBE is different for different types of cells (e.g. Tobias *et al.* 1984).
3. For shouldered survival curves, RBE depends on the survival level due to the changing curvature of the survival curves with changing LET (e.g. Barendsen *et al.* 1963).

The goal of our experiments was to measure complete sets of RBE values and to study the relation between the x-ray sensitivity of cell-lines and the RBE-LET behaviour.

2. Material and methods

2.1. Cell lines and culture conditions

V79 Chinese hamster cells were cultured in Hank's MEM medium supplemented with 10% fetal calf serum (FCS), 2 mM glutamine, 50 units/ml penicillin and 50 μg/ml streptomycin and incubated in a humidified atmosphere at 37°C and 2.0% CO₂. The cells had a cycle time of 12 h and a plating efficiency of 0.82 ± 0.11.

Chinese hamster ovary cells (CHO-K1) were grown in Ham's F12 medium, containing 10% FCS and incubated with 5% CO₂; other conditions were similar to those for V79 cells. The CHO cells had a doubling time of 12 h and a plating efficiency of 0.75 ± 0.11.

The *xrs5* mutant was derived from the CHO-K1 wild-type cell line on the basis of its hypersensitivity to x-irradiation (Jeggio and Kemp 1983). Cells were kindly provided by Dr E. Dikomey, Hamburg. The *xrs5* cells are deficient in DSB repair, due to a lack of the Ku80 component of the active DNA-PK complex (Taccioli *et al.* 1994). This plays a role in

...!!!...Lateral Scattering... !!!

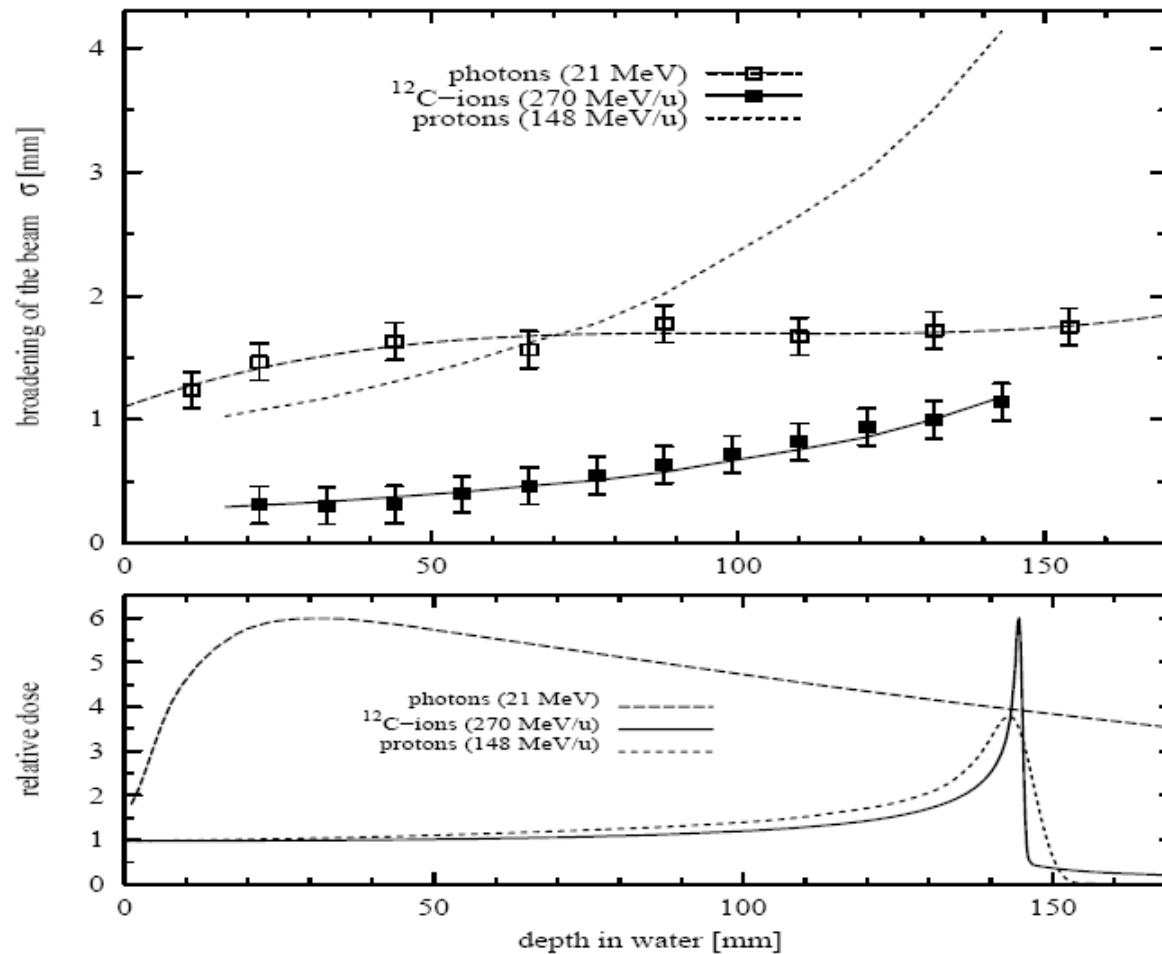


Fig. 5: Comparison of the lateral scattering of photon, proton and carbon beams as function of the penetration depth (top) and the depth dose correlation (bottom) [Weber 1996].

G. Kraft / Prog. Part. Nucl. Phys. 45 (2000) S473-S544

Fragmentation

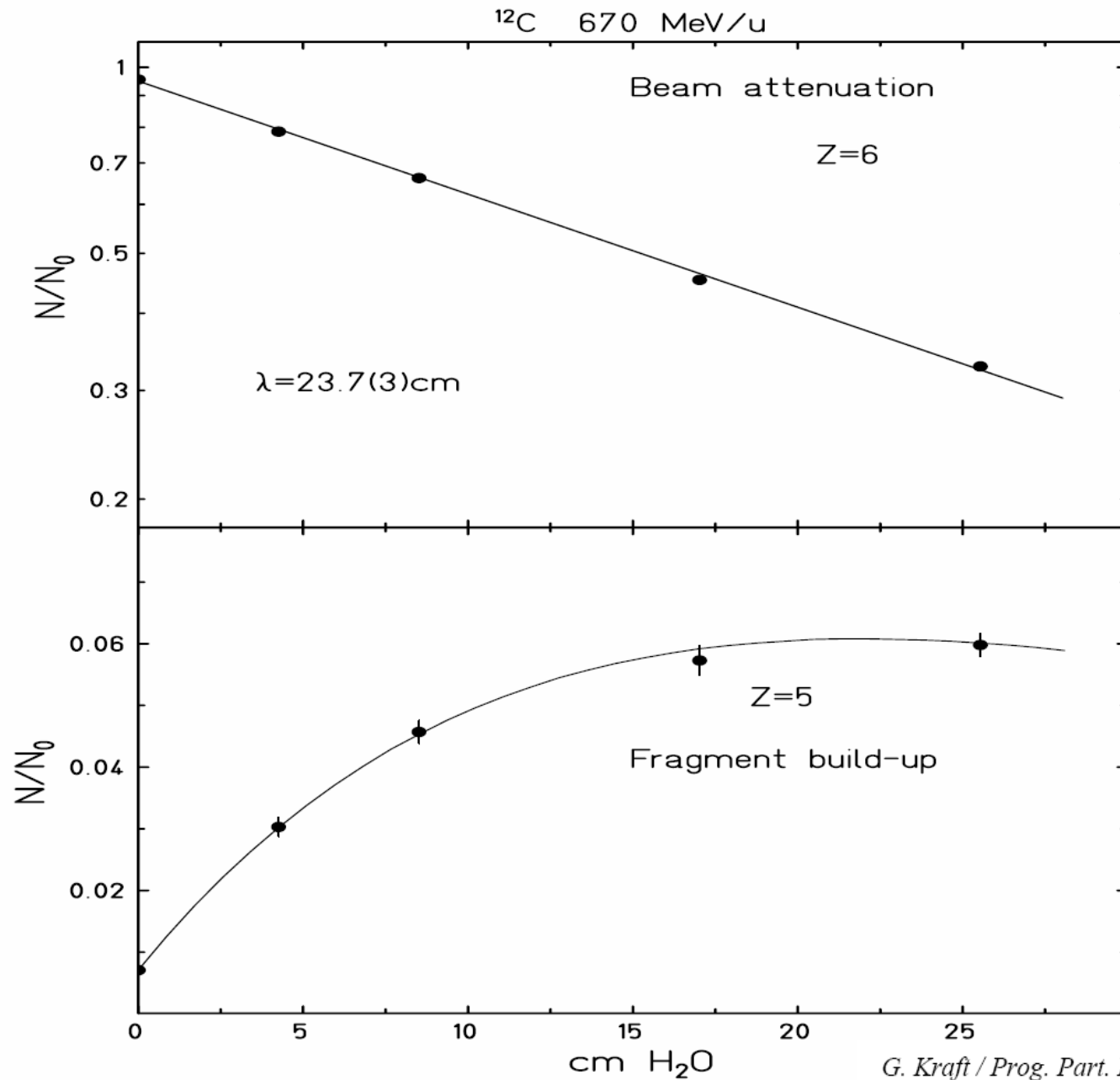


Fig. 6. Fragmentation of a 670 MeV/u carbon beam in water [Schall 1994]. Top: attenuation of the primary carbon beam as function of the penetration depth yielding a mean free path length $\lambda = 23.7$ cm. Bottom: Build up of Boron ion fragments. Because of further fragmentation to lighter ions the intensity of Boron levels off for larger penetration depths. [Schall 1996]

G. Kraft / Prog. Part. Nucl. Phys. 45 (2000) S473-S544